

DESIGN AND IMPLEMENTATION OF A
100KHz GYRATOR BAND-PASS FILTER

by

GEORGE VRETOS

A MAJOR TECHNICAL REPORT

in

THE FACULTY OF

ENGINEERING

Presented in Partial Fulfilment of the Requirement
for the Degree of Master of Engineering

at

Concordia University

Sir George Williams Campus

Montreal, P.O., Canada

March 1981

© George Vretos, 1981

ABSTRACT

DESIGN AND IMPLEMENTATION OF A
100KHZ GYRATOR BAND-PASS FILTER

George Vretos

In this report, the design and implementation of high-Q, bandpass filters using gyrators is reviewed. Chapter 1 describes passive band-pass filter synthesis, since this is the basis of the gyrator filter design procedure. Chapter 2 described the various imperfections of operational amplifiers. Chapter 3 describes the theoretical analysis of gyrator behaviour, and finally, Chapter 4 describes the implementation of a specific band-pass filter using gyrators instead of inductors. The results show that with adequate design precautions, gyrators can be used to design band-pass filters centered at 100KHz.

TABLE OF CONTENTS

	<u>PAGE</u>
ABSTRACT	
INTRODUCTION	1
CHAPTER 1: PASSIVE LC BAND-PASS FILTERS	3
1.1 Introduction	3
1.2 Specifications of the filter	4
1.3 Low-pass to band-pass transformations	6
1.4 Ideal transformers	8
CHAPTER 2: INDUCTANCE SIMULATION	16
2.1 Introduction	16
2.2 Properties of active networks (general)	16
2.3 Operational amplifiers: general	18
2.4 Nonideal operational amplifiers	21
2.5 Other imperfections of nonideal operational amplifiers	25
2.6 Minimization of parasitic effects	27
CHAPTER 3: GYRATORS	29
3.1 Introduction	29
3.2 Analysis of ideal gyrators using operational amplifiers	30
3.3 Simulation of multi-inductor networks	31
3.4 Voltage and current handling capability of gyrators	34
3.5 Analysis of nonideal gyrators	36
3.6 AC behaviour	38
3.7 Effects of finite operational amplifiers gain.	47
CHAPTER 4: IMPLEMENTATION AND TUNABILITY OF BAND-PASS FILTER	53
4.1 Introduction	53
4.2 Band-pass filter using gyrators	53
4.3 Tuning the band-pass filter	57
4.4 Parasitic effects	59
CONCLUSIONS	64
REFERENCES	65

INTRODUCTION

The unsuitability of inductors for the microelectronic realization of filters has led to the development of active RC circuits which simulate inductors. Over the period of the past twenty years, many attempts have been made to design and construct inductorless high quality filters. One of these achievements was to replace each inductor in a conventional LC ladder filter by a circuit that simulates an inductor, i.e. a capacitively-loaded gyrator.

The gyrator is an element that until few years ago had an available, if incomplete theory, but (at least at frequencies below the microwave range) only inadequate realizations. In the last years, however, several good realizations have appeared in literature, so that the gyrator now becomes available as a practical active element.

The major drawback for gyrators' performance is the effect of operational amplifier imperfections, which can be described by parasitic elements in the equivalent circuits. Because of these parasitic elements, the performance of the active filters may deteriorate considerably. Suitable steps for increasing the useful frequency range of active filters and for avoiding deterioration of its transfer performance are:

- a) Optimal design of the nonideal gyrator
- b) Incorporation of the parasitic elements into the LC structure

CHAPTER 1

PASSIVE LC BAND-PASS FILTERS

1.1 Introduction

In theory, coupled LC filters have the lowest sensitivity to component variation. These doubly terminated reactive two-ports produce a frequency response by reflecting power back to the source in the stopbands, while in the pass band, power transfer is maximum at the zero loss frequencies determined by the filter's transfer function.

In reality, a change in any component of the filter can only cause a reduction in the load power, down from the maximum. This power loss at each of the zero loss frequencies increases while at other frequencies a small loss exists because of the ripple caused by reflected power. At any point within the passband, then, the change in loss have a well behaved and slowly varying characteristic that follows the changes of any component (inductor or capacitor) in the network.

The synthesis of these networks has been studied extensively by many pioneers in this field using mathematical models, which approximate a certain transfer function to a permissible error tolerance. The results of their work are tabulated in mathematical tables to facilitate the solution of certain filter requirements.

The most commonly used filter approximations are the Butterworth, Chebyshev, and elliptic approximations. In this report the Chebyshev approximation is used.

- c) Compensation of the parasitic elements (i.e. parasitic capacitance).

In the present report the Antoniour type gyrator was investigated. This gyrator circuit has been incorporated into a band-pass filter and satisfactory results were obtained, after optimization, for a center frequency of 100KHz.

1.2 Specifications of the Filter

The required band-pass filter should have a center frequency of 100KHz, bandwidth of 20KHz, (passband edges $f_1=90\text{KHz}$, $f_2=110\text{KHz}$) with 0.1db band-pass ripple, and transmission loss, at frequencies $f_A=40\text{KHz}$, and $f_B=160\text{KHz}$ equal to or more than 40.db.

With the above specifications for the filter's performance, we first derive a prototype lowpass LC ladder network which meets the specifications. Then we transform the low-pass prototype to a band-pass filter, and substitute each individual inductance with a gyrator, terminated by a capacitance to simulate the exact value of this inductance.

This technique is superior to other techniques used, because we get filters with very low sensitivities, provided that gyrators used are optimized for low sensitivity.

From Ref. [1] we see that a third order low-pass prototype filter (Chebyshev) will meet the requirements. The prototype low-pass filter is given by Ref. [1] as shown in Fig.

1.1 The cutoff frequency of this filter occurs at $\Omega=1$.

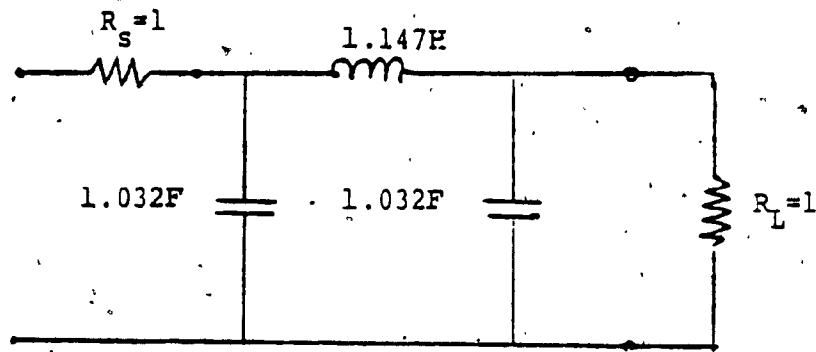


Fig. 1.1

Chebyshev low-pass prototype, 0.1 db ripple

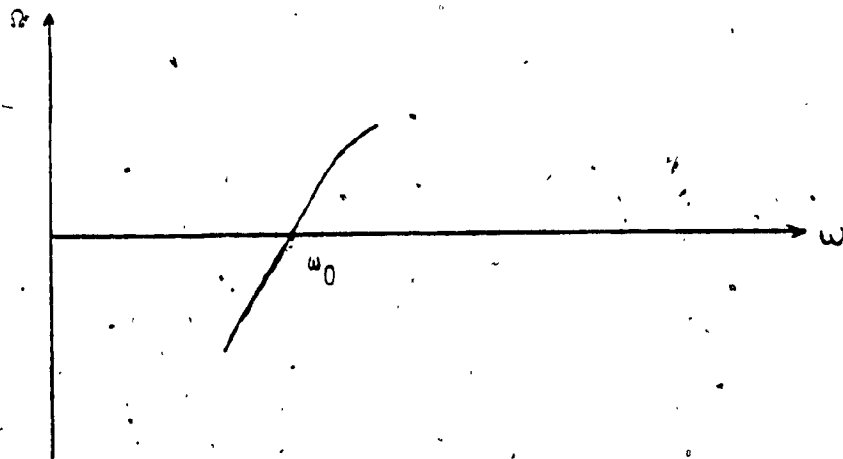


Fig. 1.2 (a)

Variation of Ω with respect to ω

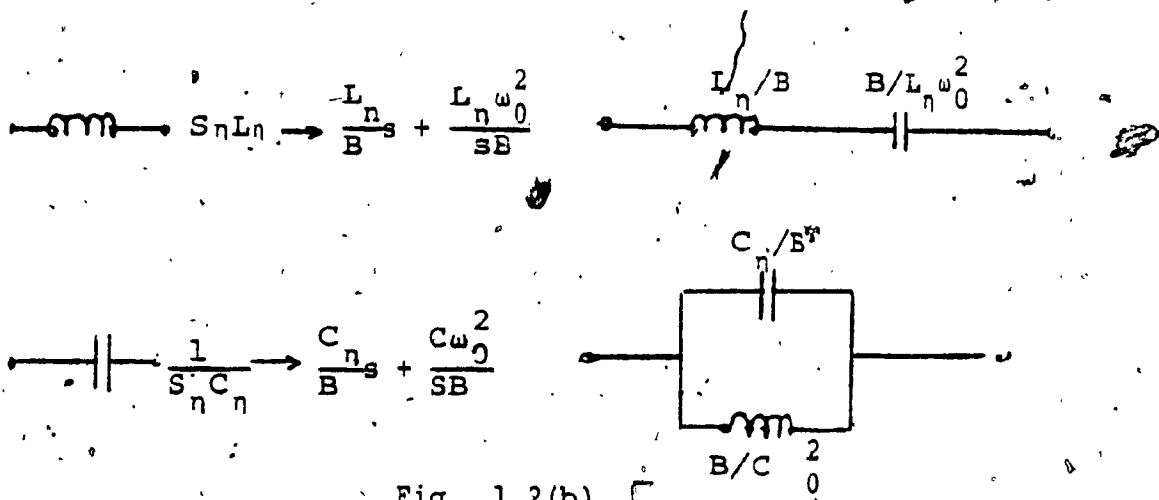


Fig. 1.2(b)

Elements transformation from low-pass to band-pass

Alternatively for $\Omega=1$, the corresponding cut-off frequency is given by:

$$\omega_2 = \frac{B}{2} + \sqrt{\frac{B^2}{4} + \omega_0^2} \quad (1.6)$$

Also from equation 1.3, we see that the region $-1 < \Omega < 1$ corresponds to:

$$\begin{aligned} \omega_1 < \omega < \omega_2 \\ \text{and} \\ -\omega_2 < \omega < -\omega_1 \end{aligned} \quad (1.7)$$

Therefore, for $\omega > 0$, the passband corresponds to

$$\omega_1 < \omega < \omega_2 \quad (1.8)$$

and the region outside corresponds to the stopband. The bandpass of the filter is given by:

$$B = \omega_2 - \omega_1 \quad (1.9)$$

Also we have

$$\omega_0^2 = \omega_1 \omega_2 \quad (1.10)$$

That is, the "centre frequency" ω_0 is the geometric mean of the lower and upper pass-band frequencies. Thus the transformation yields a filter having geometric symmetry [2]. The elements L, C, in the lowpass filter are transformed to series or parallel resonance circuits in the band-pass filter as shown in Fig. 1.2(b).

Applying the above transformation to the low-pass prototype filter Fig. 1.1, the required band-pass filter shown in

1.3 Low-pass To Band-pass Transformation

The band-pass filter structure is derived by transforming the basic normalized low-pass filter. The transformation applied on the normalized low-pass filter is

$$S_n = \frac{S^2 + \omega_0^2}{SB} = \frac{\omega_0}{B} \left(\frac{S}{\omega_0} + \frac{\omega_0}{S} \right) \quad (1.1)$$

whose cut-off frequencies are $\Omega = \pm 1$

Is $S = j\omega$ we get

$$S_n = j\Omega = \frac{-\omega^2 + \omega_0^2}{j\omega B} \quad (1.2)$$

or

$$\Omega = \frac{\omega^2 - \omega_0^2}{\omega B} \quad (1.3)$$

The variation of Ω with respect to ω is as shown in Fig. 1.2(a).

For $\Omega = -1$

we get

$$\omega^2 + B\omega - \omega_0^2 = 0 \quad (1.4)$$

or

$$\omega = -\frac{B}{2} \pm \sqrt{\frac{B^2}{4} + \omega_0^2} \quad (1.4a)$$

and for the region $\omega > 0$, the cut off frequency ω_1 is given by:

$$\omega_1 = -\frac{B}{2} + \sqrt{\frac{B^2}{4} + \omega_0^2} \quad (1.5)$$

Fig. 1.3 is derived. Impedance scaling can now yield the filter of Fig. 1.4 where $R=R_S=R_L=10K$.

From Fig. 1.4 the design values of the filter are:

$$C_1 = \frac{C_n}{RB} = \frac{1.032}{10^4 \times 20 \times 10^3} = 5,160 \text{pF} \quad (1.11)$$

$$L_1 = \frac{BR}{C_n \omega_0^2} = \frac{20 \times 10^3 \times 10^4}{1.032 (2\pi \times 100 \times 10^3)^2} = 490.897 \mu\text{H} \quad (1.12)$$

$$L_2 = \frac{L_n R}{B} = \frac{1.147 \times 10^4}{20 \times 10^3} = 573.5 \text{mH} \quad (1.13)$$

$$C_2 = \frac{B}{L_n R \omega_0^2} = \frac{20 \times 10^3}{1.147 \times 10^4 (2\pi \times 100 \times 10^3)^2} = 4.4168 \text{pF} \quad (1.14)$$

$$L_3 = \frac{BR}{C_n \omega_0^2} = \frac{20 \times 10^3 \times 10^4}{1.032 (2\pi \times 100 \times 10^3)^2} = 490.897 \mu\text{H} \quad (1.15)$$

$$C_3 = \frac{C_n}{RB} = \frac{1.032}{10^4 \times 20 \times 10^3} = 5,160 \text{pF} \quad (1.16)$$

1.4 Ideal Transformations

From the design values of the band-pass filter we see that some elements are too small, and consequently not realizable. One possible way to overcome this disadvantage is the use of ideal transformers. From Ref. 3, "The ideal transformer is a device which has zero leakage inductance, and infinite primary and secondary inductances, but so proportioned that their ratio is finite number". The voltage-current relationships are shown in Fig. 1.5.

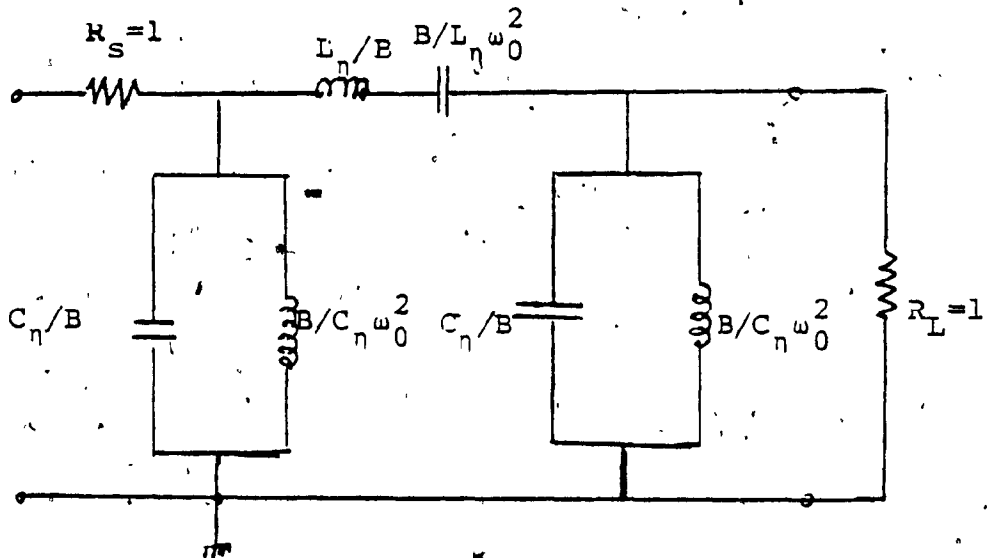


Fig. 1.3

Frequency transformation of band-pass filter derived from low-pass prototype

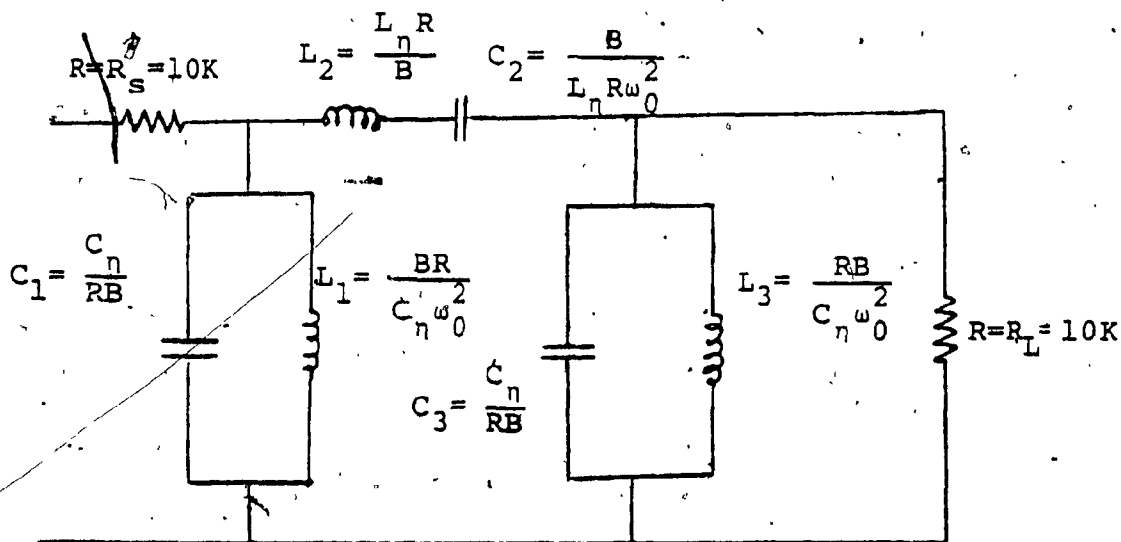


Fig. 1.4

Impedance scaling of band-pass filter

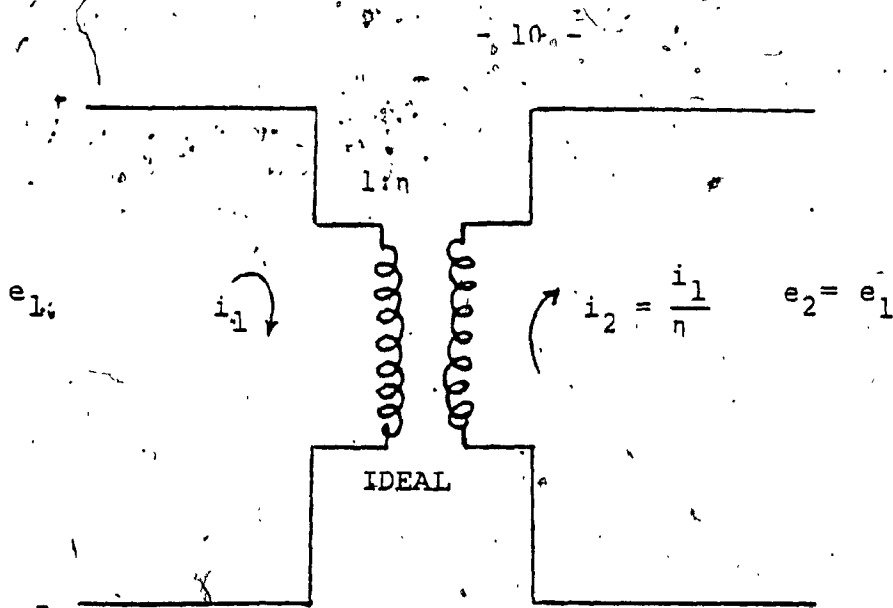


Fig. 1.5

Ideal Transformer

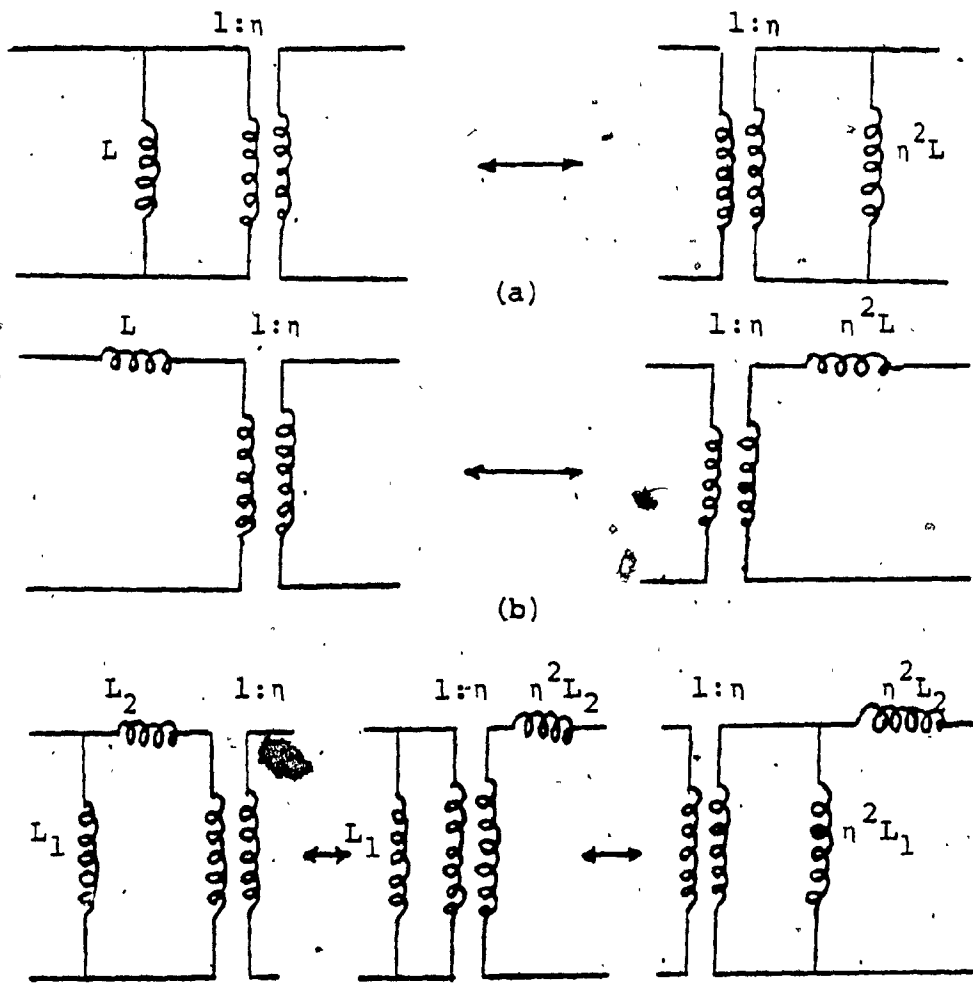


Fig. 1.6

Equivalent Circuits of Transformer

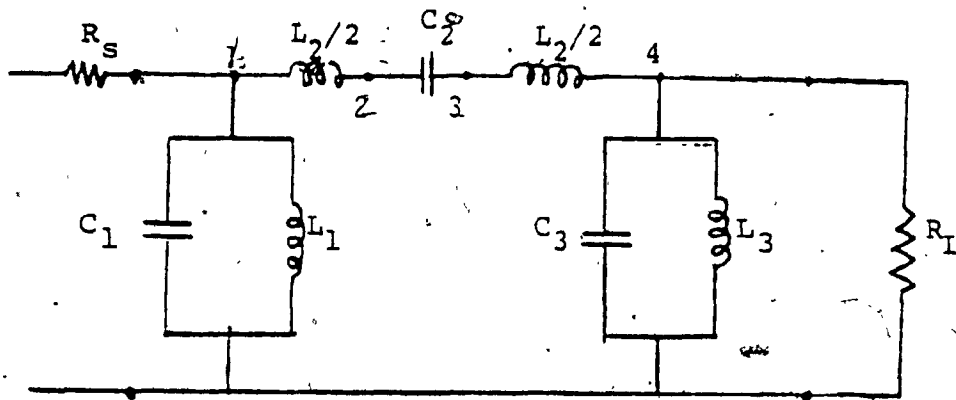


Fig. 1.7

Symmetrical band-pass filter

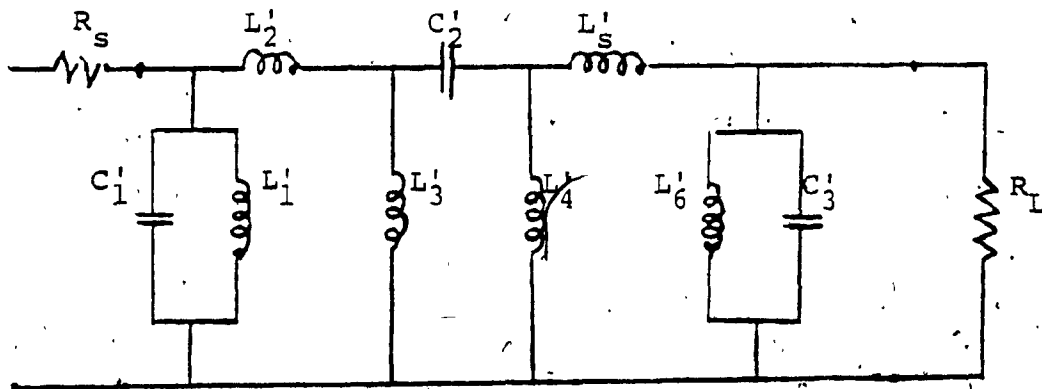


Fig. 1.8

Band-pass filter after modification

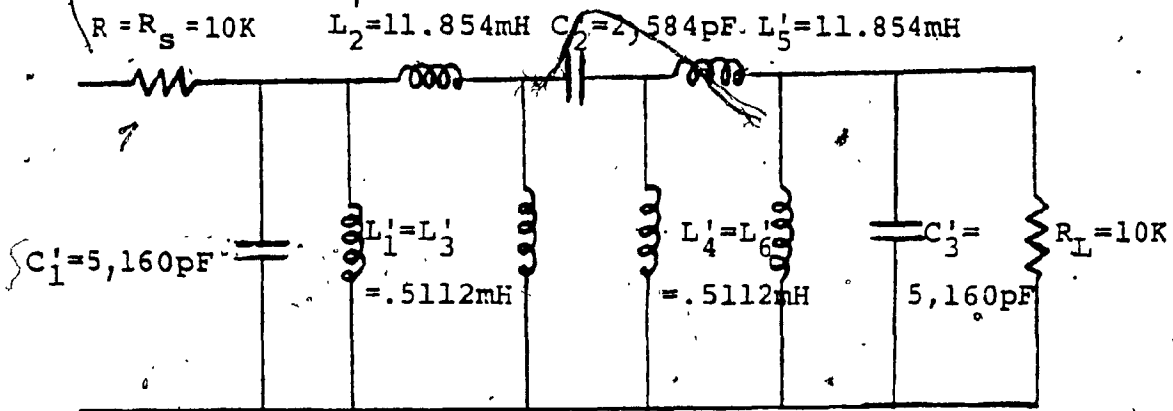


Fig. 1.9

Band-pass filter with actual values

From Fig. 1.5 we see that the volt-amperes in primary and secondary are equal, but the voltage to current ratios differ.

Since $e_2/i_2 = n^2 e_1/i_1$, and inductance in the secondary is like having an inductance $1/n^2$ times as large placed in the primary, as far as the primary is concerned. This is valid also for resistance R and capacitance C. Equivalent circuits for a transformer are shown in Fig. 1.6.

Modifying Fig. 1.4 as shown in Fig. 1.7 we get the determinant Δ for nodes 1,2,3,4 as follows.

$$\Delta = \begin{vmatrix} SC_1 + \frac{1}{SL_1} + \frac{2}{SL_2} & -\frac{2}{SL_2} & 0 & 0 \\ -\frac{2}{SL_2} & \frac{2}{SL_2} + SC_2 & -SC_2 & 0 \\ 0 & -SC_2 & SC_2 + \frac{2}{SL_2} & -\frac{2}{SL_2} \\ 0 & 0 & -\frac{2}{SL_2} & SC_3 + \frac{1}{SL_3} + \frac{2}{SL_2} \end{vmatrix}$$

The network of Fig. 1.7 has been made symmetric by splitting the series inductance L_2 into two equal inductances. From matrix theory we know that if we multiply all the elements of a row or column by a real positive number n , then the determinant Δ is multiplied by n i.e. $n\Delta$, $n\Delta_{11}$, $n\Delta_{1k}$, $n\Delta_{kk}$... etc. But since the input, output and transfer immittances are the ratios of two determinants, they do not change because the factor n cancels. In other words, if the first and last rows and columns are unchanged, the terminal conditions are unchanged, despite the manipulations of the other rows and columns.

For the above determinant Δ the second and third rows and columns can be manipulated without changing the terminal conditions. Our aim is to develop a symmetrical network which will make easier the realization of the network from the components point of view. This is done by multiplying the second and third rows and columns by n . The resultant determinant is:

$$\Delta = \begin{vmatrix} sC_1 + \frac{1}{sL_1} + \frac{2}{sL_2} & -\frac{2n}{sL_2} & 0 & 0 \\ -\frac{2n}{sL_2} & \frac{2n^2}{sL_2} + s_n^2 L_2 & -sn^2 C_2 & 0 \\ 0 & -s_n^2 C_2 & sn^2 C_2 + \frac{2n^2}{sL_2} & -\frac{2n}{sL_2} \\ 0 & 0 & -\frac{2n}{sL_2} & sC_3 + \frac{1}{sL_3} + \frac{2}{sL_2} \end{vmatrix}$$

With the information given by Figs. 1.5 and 1.6 and the small modification of Fig. 1.4 as shown in Fig. 1.7, we get the equivalent circuit of Fig. 1.8. In Fig. 1.8 we managed to shorten the gap between elements and to make the band-pass filter realizable. One should note that the source and load impedances are not affected [22].

Since transformers are not desirable elements, especially in active filters, they are replaced by equivalent circuits [3]. Each transformer can be replaced by, either an inductive or capacitive circuit. In Fig. 1.8 transformers are replaced by inductive circuits, and we see that the circuit has reduced element value disparities.

To get equal values for shunt inductances we set

$$\frac{L_1 L_2}{2L_1(1-n) + L_2} = \frac{L_2}{2n(n-1)} \quad \text{or}$$

$$2n(n-1)L_1 L_2 = 2L_2 L_1(1-n) + L_2^2 \quad \text{or}$$

$$2n^2 L_1 L_2 - 2n L_1 L_2 = 2L_1 L_2 - 2n L_1 L_2 + L_2^2 \quad \text{or}$$

$$2n^2 L_1 L_2 = 2L_1 L_2 + L_2^2 \quad (1.17)$$

$$n^2 = \frac{2L_1 L_2 + L_2^2}{2L_1 L_2} = 1 + \frac{L_2}{2L_1} \quad (1.18)$$

$$\eta = \sqrt{1 + \frac{L_2}{2L_1}} = 24.189558 \quad (1.19)$$

Therefore

$$L'_1 = L'_3 = L'_4 = L'_6 = \frac{L_2}{2\eta(\eta-1)} = 0.511278 \text{ mH} \quad (1.20)$$

$$L'_2 = L'_5 = \frac{L_2}{2\eta} = 11.854288 \text{ mH} \quad (1.21)$$

$$C'_2 = \eta^2 C_2 = 2,584.00 \text{ pF} \quad (1.22)$$

$$C_1 = C_3 = 5,160.00 \text{ pF} \quad (1.23)$$

The passive band-pass filter with actual values is shown in Fig. 1.9.

In the following chapters the simulation of the inductors by means of gyrators will be studied.

CHAPTER 2

INDUCTANCE SIMULATION

2.1 Introduction

An ideal inductor satisfies the first order, linear differential equation [7] $V = L \frac{dI}{dt}$, where L is the inductance in Henrys.

Therefore any two-terminal device that satisfies the above equation, can replace the inductor. Now if we compare the above equation with the equation for a capacitor, ie. $(I_c = C \frac{dV}{dt})$ we see that the roles played by voltage and current are reversed [8], and to simulate an inductance with a capacitor we must transform the current I to a voltage V_L and the voltage V_c to a current I_L . This is possible because both elements (inductor, capacitor) are storage elements. The two-port device that can be used to perform this conversion is a "lossless" device and is referred to as a gyrator, as defined by Tellegen [9].

2.2 Properties of Active Networks

ACTIVITY AND PASSIVITY: A network is said to be passive if, for all admissible pairs (v, i) (see Fig. 2.1) and all real $t > -\infty$

$$\int_{-\infty}^t V(\tau) i(\tau) d\tau \geq 0 \quad (2.1)$$

assuming that at $t = -\infty$, the network was relaxed and that

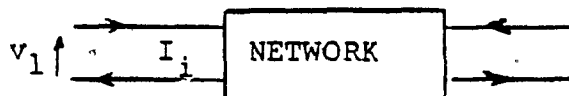


Fig. 2.1

Sign conventions for voltages and currents

the admissible signal pair in the above equation is consistent with this. This equation states that the total energy delivered to the network can never be negative for passive networks. Activity then, can be defined as the opposite of passivity. That is, a network which is not passive is active.

STABILITY: Stability can be expressed by two very useful definitions for active filters as follows [12]:

- (A) A given network is said to be marginally stable or simply stable if all voltages and currents remain bounded when all independent generators are set to zero. Otherwise it is unstable.
- (B) A given network is said to be strictly stable if all voltages and currents tend to zero as $t \rightarrow \infty$, if they are initially finite and all independent generators are then set to zero.

In active filter theory another important definition for stability is the short-circuit and open-circuit stability. A network is said to be short-circuit stable if it is stable when the ports are short-circuited. Similarly, this applies for open-circuit stability.

SENSITIVITY: Network sensitivity is of particular concern with active filters, since most of them are more sensitive to element variations than are classical filters. A measure S of sensitivity of a network to a component value K must give an indication of the change in some performance

characteristic P to variations of the component about its nominal value K_0 .

Sensitivity measures may be divided broadly into two classes, namely microscopic and macroscopic. Microscopic measures take into account only infinitesimal variations of K about its nominal value. If infinitesimal sensitivity measures may lead to incorrect results (microscopic) when elements with finite tolerances are used, then macroscopic measures should be used [12].

These properties apply if an active network (in our case filter) is well designed and optimized properly.

2.3 Operational Amplifiers

The operational amplifier is the most widely used active device of all linear circuits in production today. It is called "operational amplifier" because operations like inversion, summation, integration, etc., are readily performed when these amplifiers are used with RC networks. The most commonly used operational amplifiers are monolithic integrated circuits. These were in fact the first linear integrated circuits to be widely used. Circuit techniques used in integrated operational amplifiers are continually being modified and have many variants.

An ideal operational amplifier has two input ports. One is between the negative terminal and ground, and the other

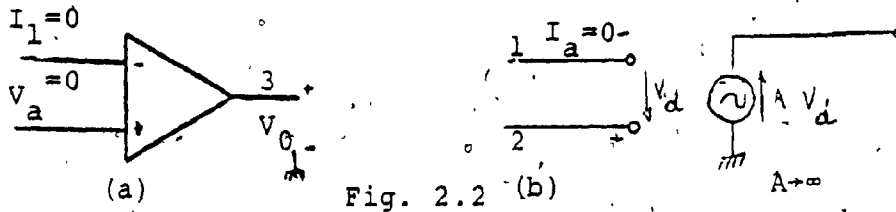


Fig. 2.2 (b)

Schematic presentation Equivalent circuit
The Ideal Operational Amplifier

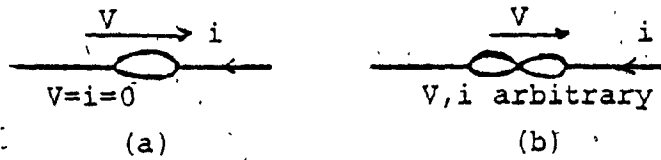


Fig. 2.3

(a) Nullator (b) Norator

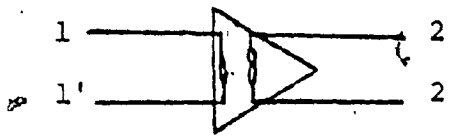


Fig. 2.4

Nullor



Fig. 2.5 (b) Open circuit condition

(a) Short circuit condition

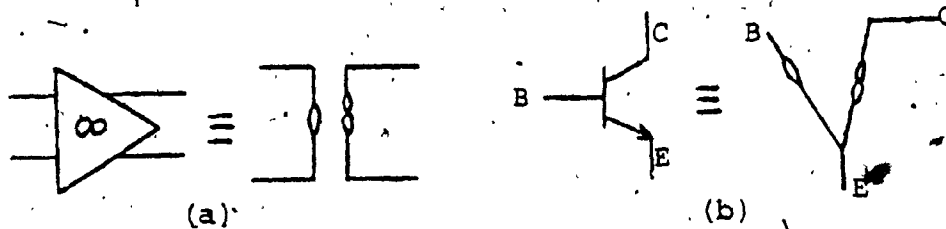


Fig. 2.6

(a) Nullor representation of the ideal op. amplifier
(b) Nullor representation of a transistor..

in different parts of an electrical network".

Fig. 2.5 shows an example of "electrical conditions".

It has been shown in the past that an ideal transistor is equivalent to a nullor. Also a nullor is equivalent to an infinite-gain voltage-controlled voltage source (V.C.V.S.) as shown in Fig. 2.6. Also it is equivalent to all the other types of infinite gain controlled sources.

The manipulation of nullators and norators simplifies the analysis and synthesis of active networks, and presents a better understanding of a given or new derived active network. These two elements exist only as paper elements and it is not possible to approximate them in practice. Therefore they must be used with care in analysis and synthesis of active networks.

2.4 Nonideal Operational Amplifiers

A practical operational amplifier differs from the ideal one shown in Fig. 2.2, in that gain and input impedance are finite, and that the output impedance is not zero. The equivalent circuit of a practical differential input operational amplifier is given in Fig. 2.17 [31].

The differential voltage gain A of the amplifier is defined by

$$A = \frac{E_O}{E_N - E_I} \quad (2.2)$$

between the positive terminal and ground. It has only one output port, the voltage across which is shown as V_o (Fig. 2.2).

When operating in the linear region, the operational amplifier has the following characteristics [11]:

1. It has infinite impedance at both input ports.
2. It has infinite gain.
3. It has zero output impedance.

The above three characteristics are expressed by the equivalent circuit shown in Fig. 2.2.

A better concept of operational amplifiers can be achieved by using nullors [13]. A nullor consists of two singular elements as shown in Fig. 2.4. These two singular elements are shown in Fig. 2.3 and were described by Carlin and Youla.

Fig. 2.3(a) represents a "pathological" one-port singular element for which the voltage across and the current through are simultaneously constrained to be zero. Such a one-port is called a nullator. Fig. 2.3(b) represents a "pathological" one port defined by the dual relations:

$$V = \text{arbitrary}, \quad i = \text{arbitrary}$$

and known as a norator. The values of the electrical variables for this singular element, are established by the rest of the circuit in which it is embedded [15]. In reality these two singular elements represent "electrical conditions

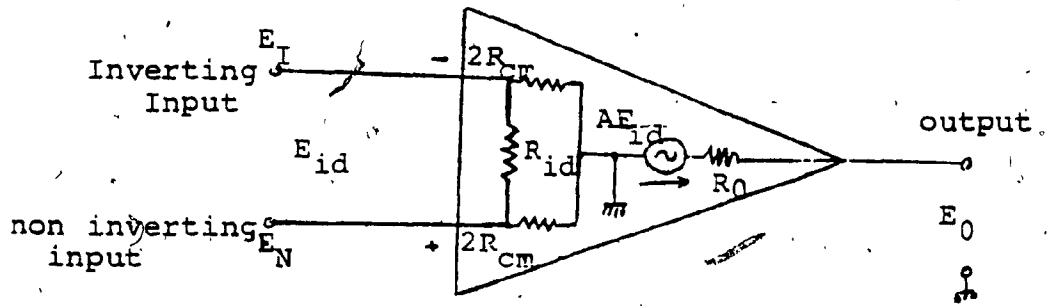


Fig. 2.7

Non-ideal operational amplifier

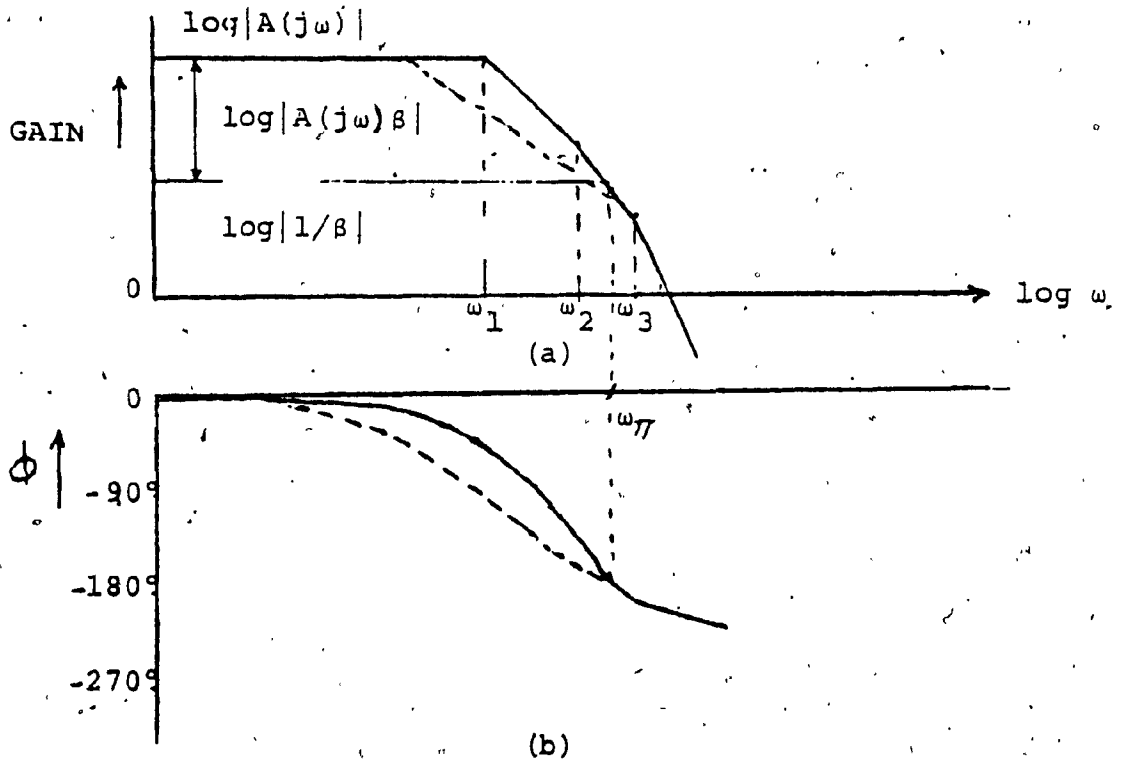


Fig. 2.8

Amplitude $|A(j\omega)|$ and phase shift ϕ of the amplifier

Where

E_N - voltage at the non-inverting input

E_I - voltage at the inverting input

The differential input voltage is defined as

$$E_{id} = E_N - E_I \quad (2.3)$$

The differential input resistance R_{id} is generally in the range of 100K to 10^6 M Ω . In addition to this, there is common-mode resistance $2R_{cm}$ from each of the two inputs to ground. The value of R_{cm} is very high, generally ranging from 10^7 to 10^8 M Ω . Since the common-mode input resistance R_{cm} is much larger than the differential input resistance, the effect of R_{cm} can be neglected for most practical applications. The output resistance R_o of the amplifier is low, generally ranging from a few ohms to 1 K Ω .

Practical operational amplifier circuits may be classified in many ways, but perhaps the most useful is by the number of stages within the amplifier providing voltage gain. This system of classification is useful, because the voltage gain stages tend to contribute the dominant poles of the differential voltage gain function of the circuit, and hence dictate the amount and type of frequency compensation which must be used [35].

The finite but high open-loop gain is obtained by cascading several stages, and the gain of each stage starts falling

off at 6db/octave after a certain frequency. Thus the net roll-off of the total gain can be as high as 18db/octave. According to Bode's stability criterion, the rate of closure between the open-loop and the closed-loop response must be less than 12db/octave.

With a given operational amplifier it is usually not possible to apply arbitrary amounts of feedback to achieve a given closed-loop gain, unless the open-loop phase shift is corrected with additional circuitry. The correction procedure is called "frequency compensation" or "phase compensation", although the phase-shift is actually only partially compensated in a restricted band of frequencies. The frequency compensation can be achieved externally by alteration of the external feedback, or internally by the use of additional components in the amplifier circuit. Some of the methods most often used are called "lag compensation", "lead-lag compensation", "feed-forward compensation".

A reasonable approximation of the open-loop gain for a practical operational amplifier is given by

$$A(s) = \frac{A_0}{\left(1 + \frac{s}{\omega_1}\right) \left(1 + \frac{s}{\omega_2}\right) \left(1 + \frac{s}{\omega_3}\right)} \quad (2.4)$$

where $0 < \omega_1 < \omega_2 < \omega_3$. The approximate (asymptotic) behaviour of $\log |A(j\omega)|$ as a function of $\log \omega$ is shown in Fig. 2.8 in the

form of a Bode diagram. $|A(j\omega)|$ is constant for $\omega < \omega_1$. It falls off at 6db/octave between ω_1 and ω_2 , at 12db/octave between ω_2 and ω_3 , and at 18db/octave above ω_3 [33].

The phase shift ϕ is shown as a function of $\log \omega$, and it is given approximately by -45° , -135° , and -225° at the corner frequencies ω_1 , ω_2 , and ω_3 , respectively, assuming that these frequencies are well separated. From Fig. 2.8 we derive a simple sufficient criterion for a good design for an operational amplifier. The open-loop gain should not fall off at more than 12db/octave at frequencies for which $|A(j\omega)| > 1$.

2.5 Other Imperfections of Nonideal Operational Amplifier

1. Slew rate: If an operational amplifier is overdriven by a large-signal pulse, or square wave having a fast enough rise time, the output does not follow the input immediately. Instead, it ramps or "slews" at some limiting rate determined by internal currents and capacitances. The magnitude of input voltage required to make the amplifier reach its maximum slew rate varies, depending on the type of input stage used [34]. As an example, in an operational amplifier with a slew rate of $0.5V/\mu$ sec, 60μ sec are required to change the output from $-15V$ to $+15V$. For a sinewave, the slew rate is defined as

$$\text{slew rate} = 2\pi f_p V_{\text{max}} \quad (2.5)$$

where f_p is the maximum input frequency beyond which rated output cannot be obtained without significant distortion

V_{max} is half the (rated) output swing of the operational amplifier.

2. Power bandwidth: Power bandwidth is defined as the maximum frequency at which full output swing (usually 10V peak) can be obtained without distortion. For a sinusoidal output voltage $V_o(t) = V_p \sin \omega t$, the slew rate required to reproduce the output is

$$\frac{dV_o}{dt} = \omega V_p \cos \omega t \quad (2.6)$$

This has a maximum when $\cos \omega t = 1$, giving

$$\left. \frac{dV_o}{dt} \right|_{max} = \omega V_p \quad (2.7)$$

so the highest frequency that can be reproduced without slew limiting, ω_{max} (power bandwidth) is

$$\omega_{max} = \frac{1}{V_p} \left. \frac{dV_o}{dt} \right|_{max} \quad (2.8)$$

Thus power bandwidth and slew rate are directly related by the inverse of the peak of the sinewave V_p .

3. Unity gain bandwidth: In order to ensure stability of a practical operational amplifier when used in a unity gain configuration, the compensation capacitor must be chosen

to provide a dominant pole. This dominant pole must produce a 6db/octave roll-off in gain so that unity gain is reached at some frequency ω_T lower than the next most important pole produced by the amplifier. Thus the value of ω_T and of compensation capacitance are determined by the frequency limitations of the devices in the amplifier. The unity gain bandwidth is inversely proportional to the duration of the slew rate. Thus a principal aim in high-speed operational amplifier design, is the achievement of high gain-bandwidth product with sufficient phase margin to give an optimally damped response.

The gain bandwidth product is determined by the location of the higher frequency poles, which contribute excess phase at frequencies at and above crossover [35]. These higher frequency poles are contributed by the fall-off of the gain of the various stages within the amplifier.

2.6 Minimization of Parasitic Effects

In order to achieve good high-frequency performance with operational amplifiers it is necessary to use them with large gain-bandwidth products, rather than the more usual high-gain operational amplifiers with gain-bandwidth products of the order of 1MHz to 10MHz. In fact, the very large dc gains of the common operational amplifiers are unnecessary in most active filter applications.

Other important factors are

- a) Layout: a good layout can reduce stray capacitances and load impedances.
- b) Technological improvements: technological improvements can be relied upon to continue to reduce many parasitic effects. Also, the effects of many parasitic components can be minimized by a correct choice of the impedance level in the network. Some parasitic effects can also be minimized by choice of dc operating currents and voltages. A possible disadvantage in either case is that the dc power consumption may be increased. However, many parasitic components can be "designed in" or "swamped out". For instance, amplifier input resistances can usually be allowed for by slightly altering the design.

CHAPTER 3

GYRATORS

3.1 Introduction

An "ideal gyrator" is a two-port non-reciprocal network, which at either port, presents a driving-point impedance proportional to the terminating admittance connected across the other port, with a positive constant of proportionality [10]. This ideal gyrator is a lossless and unconditionally stable network and is described by the short-circuit admittance parameters [4]

$$Y_{11} = Y_{22} = 0 \quad (3.1)$$

$$Y_{12} = -Y_{21} = G \quad (3.2)$$

In practical gyrators instability and sensitivity problems can occur due to operational amplifier limitations. Therefore the design of a practical gyrator should be based on stability and sensitivity optimization. Direct transformation of capacitance into inductance is possible with gyrator. Therefore inductors simulated in this way can be used in the construction of very insensitive active filters [12]. Many gyrator designs and implementations can be found in the literature which exhibit good performance [16] to [20]. Gyrators can be realized by networks with resistors, capacitors and non-reciprocal components. The non-reciprocal components

This is the basic gyrator equation and can be made to show an inductive character in two ways. If Z_1, Z_2, Z_3, Z_5 are resistors and Z_4 is a capacitor in Fig. 3.1(b) the equation becomes

$$V_i = sLI_i \quad (3.7)$$

where

$$L = \frac{R_1 R_3 R_5 C_4}{R_2} \quad (3.8)$$

This will be referred to in this report as a type GA configuration. If, on the other hand, Z_1, Z_3, Z_4, Z_5 are resistors and Z_2 a capacitor as in Fig. 3.1(c) the equation becomes

$$V_i = sLI_i \quad (3.9)$$

where

$$L = \frac{R_1 R_3 R_5 C_2}{R_4} \quad (3.10)$$

This will henceforth be referred to as a type GB configuration. Whenever possible, all of the resistors are made equal for convenience, which gives $L=R^2C$ for either configuration. The term R^2 is often called the gyration constant. Consequently the circuit configurations shown in Fig. 3.1(b) and (c) convert a capacitance into an inductance.

3.3 Simulation of Multi-Inductor Networks

The circuit discussed above simulates only inductors having one end grounded, which are not suitable for many filter configurations. However, an interconnection of two gyrators

of practical interest with reference to present technology are the transistor and the operational amplifier [29]. As ideal transistors and operational amplifiers can be modelled by nullors, it has been proved in the past [5] that two nullors are necessary to realize a gyrator.

In this report, for the realization of the band-pass filter, the Antoniou GIC [5], [4] will be used and analyzed, because it has been shown to be superior to other known GIC realizations [6].

3.2 Ideal Analysis of Gyrators Using Operational Amplifiers

The circuit model developed by Antoniou is shown in Fig. 3.1 along with the definitions of the variables to be used in the analysis. In the ideal analysis the operational amplifiers are assumed to have infinite gain, infinite input impedance, zero output impedance, and zero offset. The voltages across the inputs of the amplifiers must be zero. Thus we have the equations

$$I_i Z_1 + (I_i - I_5) Z_2 = 0 \quad (3.3)$$

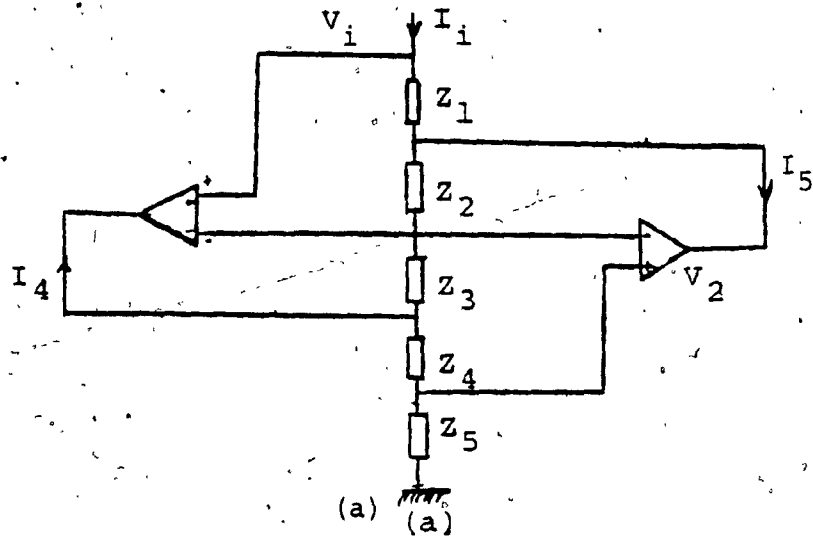
$$(I_i - I_5) Z_3 + (I_i - I_5 - I_4) Z_4 = 0 \quad (3.4)$$

Also

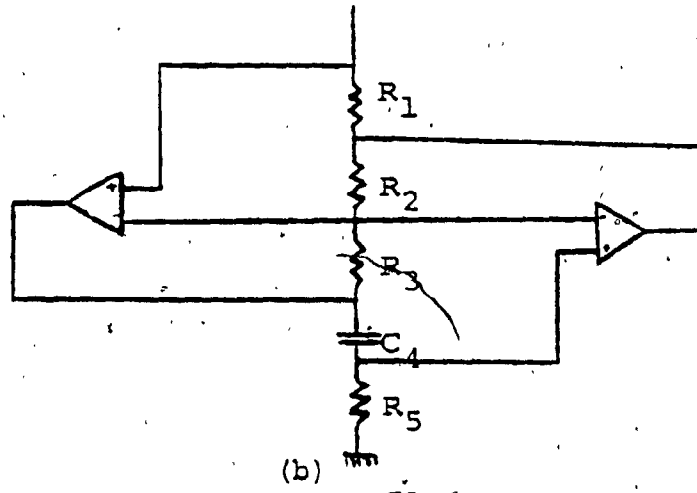
$$V_i = I_i Z_1 + (I_i - I_5) (Z_2 + Z_3) + (I_i - I_5 - I_4) (Z_4 Z_5) \quad (3.5)$$

Combining these equations yields

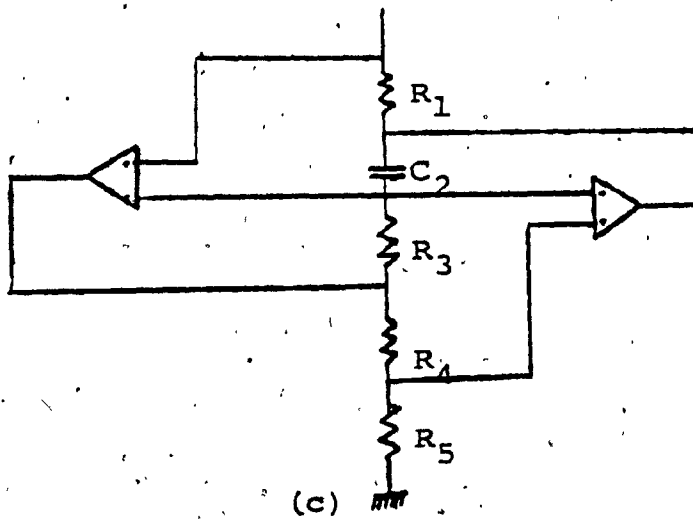
$$V_i = \left(\frac{Z_1 Z_3 Z_5}{Z_2 Z_4} \right) I_i \quad (3.6)$$



The Antoniou GIC basic



Type GA



Type GB

Fig. 3.1

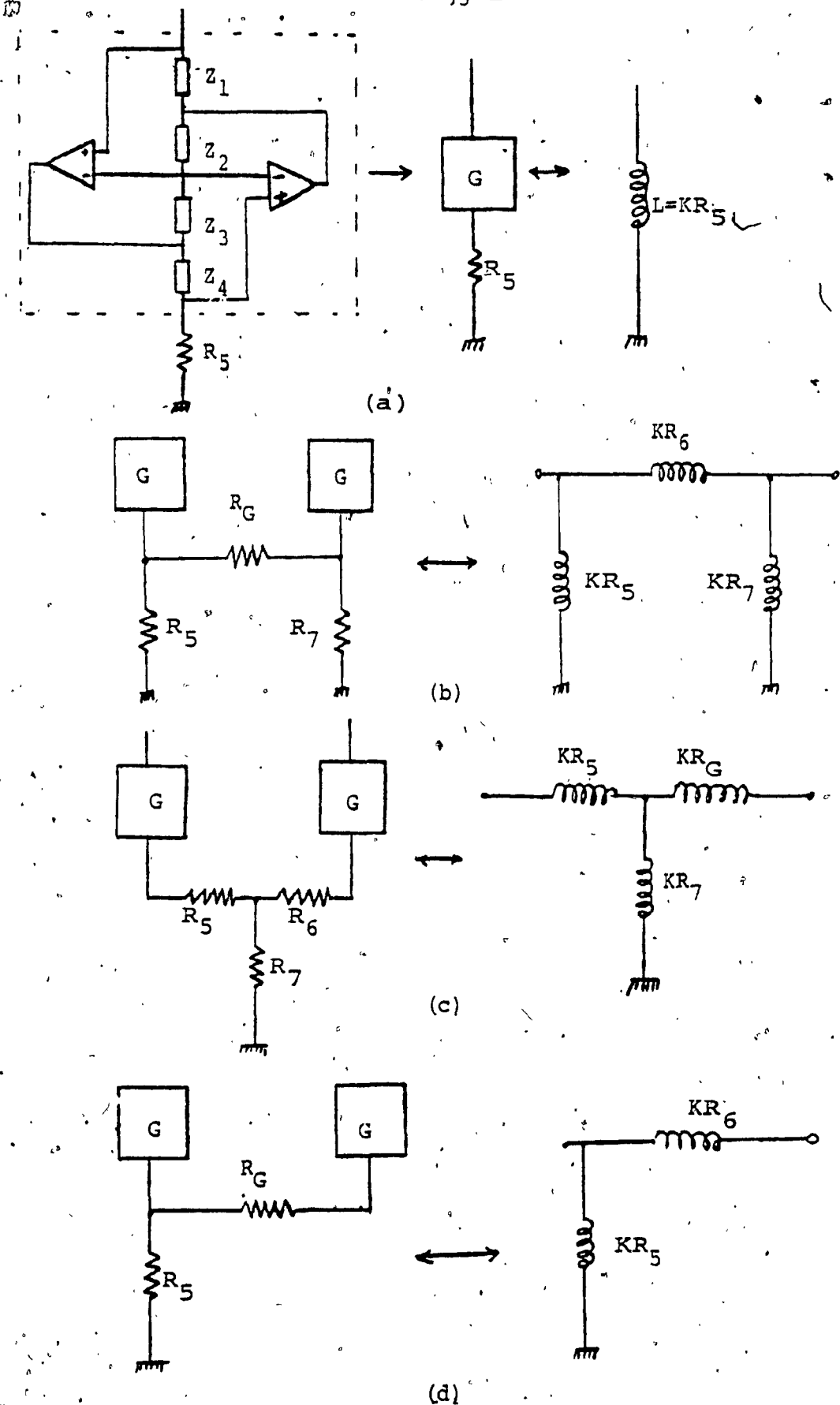


Fig. 3.2

Simulation of multi-inductor networks

Substituting the value of I_5 to equ. (3.12) we get

$$I_4 = -I_i \left(\frac{Z_1 Z_3}{Z_2 Z_4} + \frac{Z_1}{Z_2} \right) \quad (3.14)$$

The gyrator voltages are given by

$$V_1 = (I_i - I_5) Z_4 \quad (3.15)$$

$$V_2 = V_i - I_i Z_1 \quad (3.16)$$

Using the two current equations the above expressions can be simplified to

$$V_1 = V_i \left(1 + \frac{Z_4}{Z_5} \right), \quad V_2 = V_i \left(1 - \frac{Z_2 Z_4}{Z_3 Z_5} \right) \quad (3.17)$$

The amplifier currents can also be written in terms of the input voltage, as follows

$$I_4 = \frac{V_i}{Z_5} \left(1 + \frac{Z_4}{Z_3} \right) \quad (3.18)$$

$$I_5 = V_i \left(\frac{Z_2 Z_4}{Z_1 Z_3 Z_4} \right) \left(1 + \frac{Z_1}{Z_2} \right) \quad (3.19)$$

Recalling that $\frac{V_i}{I_i} = j\omega L$ and assuming a type GA gyrator, these equations can be further rewritten as

$$V_1 = V_i \left(1 + \frac{R_1 R_3}{j\omega L R_2} \right) \quad (3.20)$$

$$V_2 = V_i \left(1 - \frac{R_1}{j\omega L} \right) \quad (3.21)$$

$$I_4 = \frac{V_i}{R_5} \left(1 + \frac{R_1 R_5}{j\omega L R_2} \right) \quad (3.22)$$

$$I_5 = \frac{V_i}{j\omega L} \left(1 + \frac{R_1}{R_2} \right) \quad (3.23)$$

can simulate more general inductor networks [21], as shown in Fig. 3.2. The resistive network interconnecting the two gyrators is exactly the same as the inductive network being simulated. However, in order for these circuits to perform correctly, the corresponding impedances Z_1, Z_2, Z_3, Z_4 of each of the two gyrators must be identical. Thus each inductor is proportional to the corresponding resistor in the interconnection network.

3.4 Voltage and Current Handling Capability of Gyrators

The maximum input voltages and currents which the gyrators can handle are determined by the passive element values and the voltage and current levels at which the operational amplifiers begin to saturate.

From the basic configuration of the gyrator we will determine the operational amplifier currents. The gyrator is assumed to be ideal in this analysis.

The two current equations were found as

$$I_i Z_1 + (I_i - I_5) Z_2 = 0 \quad (3.11)$$

$$(I_i - I_5) Z_3 + (I_i - I_5 - I_4) Z_4 = 0 \quad (3.12)$$

From equation 3.11 we readily find I_5 as

$$I_5 = I_i \left(1 + \frac{Z_1}{Z_2}\right) \quad (3.13)$$

does not occur in the proposed filter configurations and estimate, if possible, the size of the output offset voltages.

The basic gyrator configuration in Fig. 3.3 will be considered first. Modifying the basic equations from the ideal analysis to include offset voltage and bias current terms gives

$$(I_i + i_1)Z_1 + (I_i + i_1 - I_5)Z_2 = e_1 \quad (3.24)$$

$$(I_i + i_1 + i_2 + i_3 - I_5)Z_3 + (I_i + i_1 + i_2 + i_3 - I_5 - I_4)Z_4 = -e_2 \quad (3.25)$$

$$V_i = (I_i + i_1)Z_1 + (I_i + i_1 - I_5)Z_2 + (I_i + i_1 + i_2 + i_3 - I_5)Z_3 + (I_i + i_1 + i_2 + i_3 - I_5 - I_4)Z_4 + (I_i + i_1 + i_2 + i_3 + i_4 - I_5 - I_4)Z_5 \quad (3.26)$$

Solution of these equations gives

$$V_i = I_i \left(\frac{Z_1 Z_3 Z_5}{Z_2 Z_4} \right) + e_1 \left(1 - \frac{Z_3 Z_5}{Z_2 Z_4} \right) - e_2 \left(1 + \frac{Z_5}{Z_4} \right) + i_1 (Z_1 + Z_2) \times \left(\frac{Z_3 Z_5}{Z_2 Z_4} \right) - (i_1 + i_2 + i_3) (Z_3 + Z_4) \left(\frac{Z_5}{Z_4} \right) + (i_1 + i_2 + i_3 + i_4) Z_5 \quad (3.27)$$

where e_1, e_2 are offset voltages and i_1, i_2, i_3, i_4 are bias currents.

Clearly if a $1/s$ term (step function) multiplied any of these constants, it would increase linearly and eventually saturate the gyrator. To illustrate the meaning of the equations, let all the gyrator resistors have a value R and the capacitor a value C . Then, for type GA gyrator we have

Knowing the maximum voltages and currents of the operational amplifiers, one can calculate the maximum input voltages before the onset of distortion. A similar set of equations can be written for a type GB gyrator. In theory, one can determine optimum gyrator element values to allow a maximum input but, in practice, this could result in unrealistic element values.

3.5 Analysis of nonideal gyrators

DC considerations:

An ideal operational amplifier should respond only to the difference in value of the signals applied to the non-inverting and inverting terminals. Unfortunately, a practical operational amplifier has both input offset voltage and input bias currents and may have noticeable effects on the circuits in which they are used [15]. Their effect on circuit behaviour should be determined. The amplifier's DC gain is very large and will be assumed infinite. DC offset at the output of a bandpass filter is not a serious problem, since the output can be AC coupled, as long as the offset is not large enough to interfere with proper circuit operation. The problem is that when the power is turned on, several of the amplifier output voltages drift slowly toward saturation. The voltages increase linearly with time and the whole process takes 5-10 sec., suggesting that a very small bias current is charging a capacitor. We must ensure that such behaviour

$$V_i = I_i (sCR^2) + e_1 (1 - sCR) - e_2 (1 + sCR) - (i_2 + i_3) (2sCR^2) + (i_1 + i_2 + i_3 + i_4) R \quad (3.28)$$

and for type GB

$$V_i = I_i (sCR^2) + e_1 (1 - sCR) - 2e_2 + i_1 (R + sCR^2) - (i_1 + i_2 + i_3) 2R + (i_1 + i_2 + i_3 + i_4) R \quad (3.29)$$

From the above equations we see that the two circuits are unconditionally stable as expected, and shown by [5].

At DC, $s=0$, and so we conclude that

$$\text{Offset voltage (type GA)} = e_1 - e_2 + (i_1 + i_2 + i_3 + i_4) R \quad (3.30)$$

$$\text{Offset voltage (type GB)} = e_1 - 2e_2 + (i_4 - i_2 - i_3) R \quad (3.31)$$

For typical operational amplifiers, e_1 and e_2 are around 5mV and each of the bias currents are of the order of 100-200nA. From the above equations we conclude that the gyrator produces a steady offset voltage independent of the load. If that load is an inductor (or another gyrator) the offset voltage will produce a rising current, limited only by the inductor's internal resistance. Such a situation should be avoided.

3.6 AC Behaviour

The nonideal AC behaviour of a gyrator is determined by the parameters of the operational amplifier. In practice, the operational amplifier is a nonideal device. It is

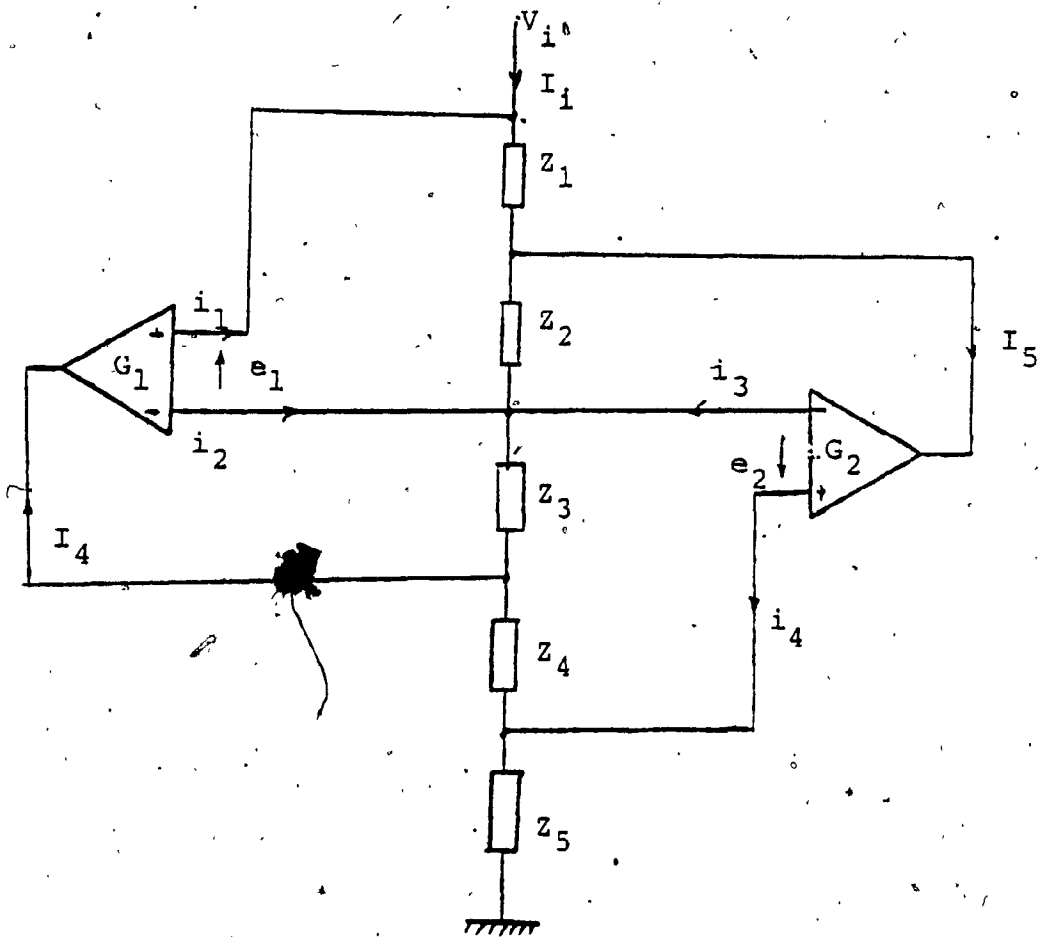


Fig. 3.3

Gyrator dc offset analysis

$$G_{P_1} = \frac{1}{R_{P_1}} + \frac{1}{A_O R} \left(2 + \frac{R_O}{R} \right) + \frac{R}{R_I (2R + 3R_O + A_O \omega_O R^2 C)} \quad (3.33)$$

$$G_{P_2} = - \left(\frac{1}{R_{N_1}} + \frac{1}{R_{N_2}} + \frac{2R_O}{R (2R + 3R_O + A_O \omega_O R^2 C)} \right) \quad (3.34)$$

$$\begin{aligned} G_{P_3} &= \frac{2\omega^2}{A_O^2 \omega_O^2 R} \left(1 + \frac{4R_O}{R} - \frac{(4RR_O R_I + 2R^2 R_O - 4R_O^2 R_I - 2R^3)}{RR_I (2R + 3R_O + A_O \omega_O R^2 C)} \right) \\ &= \frac{2\omega^2}{A_O^2 \omega_O^2 R} \left[1 + \frac{4R_O}{R} + \frac{1}{2 + \frac{A_O \omega_O R C}{R}} \left(-\frac{R_O}{R} + \frac{R}{R_I} \right) \right] \end{aligned} \quad (3.35)$$

$$\begin{aligned} C_D &= \frac{1}{A_O \omega_O R} \left[2 + \frac{R_O}{R} + \frac{1}{RR_I} \left(\frac{R_O (R_O R_I - R^2)}{2R + 3R_O + A_O \omega_O R^2 C} \right) \right] \\ &= \frac{1}{A_O \omega_O R} \left[2 + \frac{R_O}{R} \right] \end{aligned} \quad (3.36)$$

$$r_{P_4} = \frac{2R}{A_O} + \frac{3R_O}{A_O} + G_L R^2 \quad (3.37)$$

$$r_{P_5} = \frac{2\omega^2}{A_O^2 \omega_O^2} (R + 6R_O) \quad (3.38)$$

$$L_P = \frac{2R}{A_O \omega_O} + \frac{3R_O}{A_O \omega_O} \quad (3.39)$$

and

$$L_O = R^2 C \quad (3.40)$$

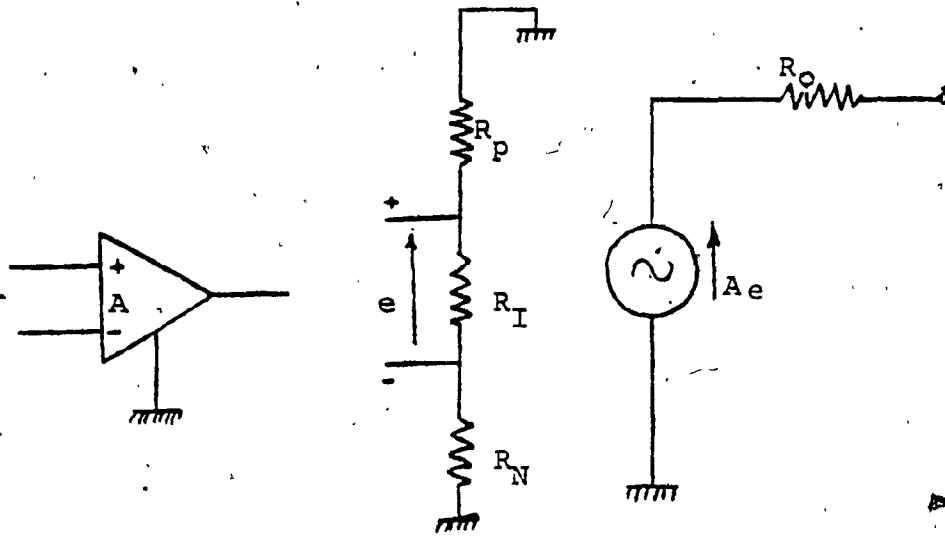


Fig. 3.4

Model for nonideal operational amplifier

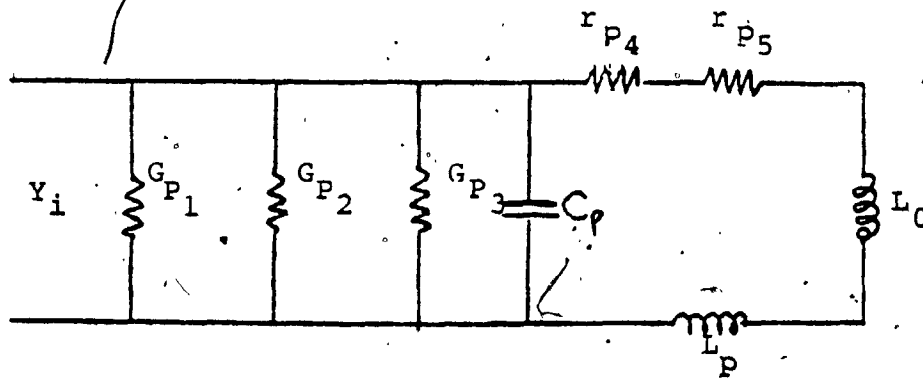


Fig. 3.5

Model for the capacitively terminated gyrator

D
and

$$\frac{\Delta M(\omega)}{M(\omega)} = \frac{1}{B} \int A(s) ds$$

for the deviation due to a finite A_0 and B , respectively.

With the above typical values we conclude that the gain-bandwidth product B is a very important parameter for frequencies above 50KHZ, because it has greater effect than the dc open-loop gain.

The basic gyrator configuration (type GA) has been modelled by [24] for non-ideal operational amplifier, shown in Fig. 3.5 (equivalent circuit) and the following parasitic elements were introduced

1. A constant series parasitic inductance L_p .
2. A constant parallel parasitic capacitance C_p (analogous to the winding capacitance in an inductor).
3. A frequency-dependent parallel resistance $1/G_{p3}$ which reduces as the frequency is increased.
4. A frequency-dependent series resistance r_{p5} which increases as the frequency is increased (analogous to the winding resistance in an inductor which increases due to the skin effect).
5. For a nonzero R_0 , enhancement is introduced.

Also, the various values of the parasitic components were given

characterized by a frequency-dependent voltage gain whose magnitude starts from a very high value at DC (usually in the range of 80 to 120db) and then monotonically decreases for higher frequencies. Likewise, the phase of the voltage gain is a monotonically decreasing function starting from 0° at dc.

The nonideal voltage transfer function $A(s)$ of the operational amplifier is usually approximated by the expression

[23]

$$A(s) = \frac{A_0 \omega_0}{s + \omega_0} \quad (A_0 \omega_0 \gg 1). \quad (3.32)$$

where A_0 is the dc open-loop gain of the operational amplifier, and ω_0 is the cut off radian frequency.

Typical values given in [24] for the parameters of the model shown in Fig. 3.4 are

$$A_0 = 3,000 - 200,000, \quad \omega_0 = 30 - 15 \times 10^3 \text{ rads/sec}$$
$$R_p, R_N : 50 - 500 \text{M}\Omega, \quad R_I : 50 \text{K}\Omega - 2 \text{M}\Omega, \quad R_O = 50 - 200 \Omega$$

Ref. [23] reports that for sufficiently small deviations $\Delta M(\omega)$ of the gain function (magnitude), the effect of finite A_0 and finite B on $M(\omega)$ are given by

$$\frac{\Delta M(\omega)}{M(\omega)} \approx - \frac{\int A(s) ds}{A_0}$$

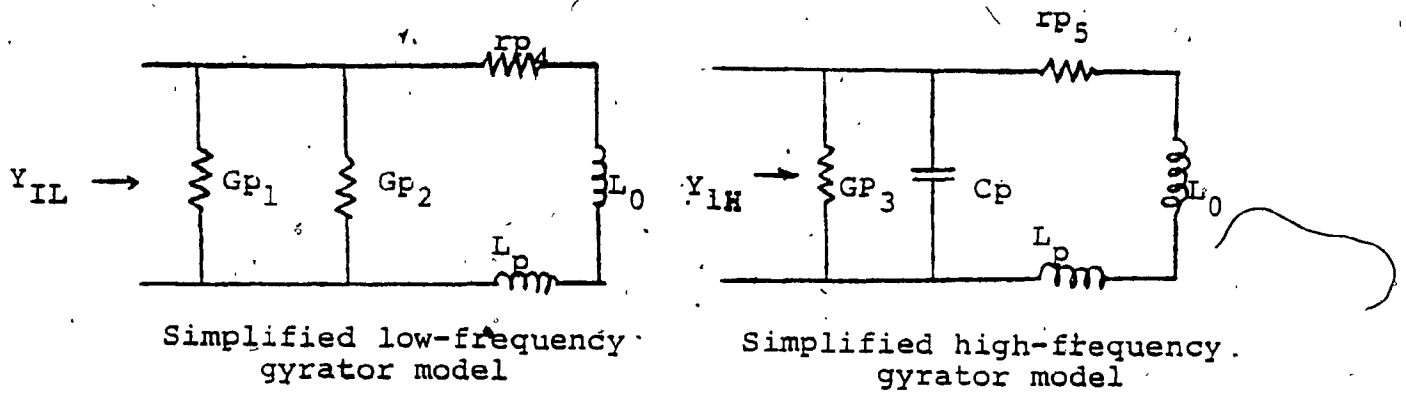


Fig. 3.6

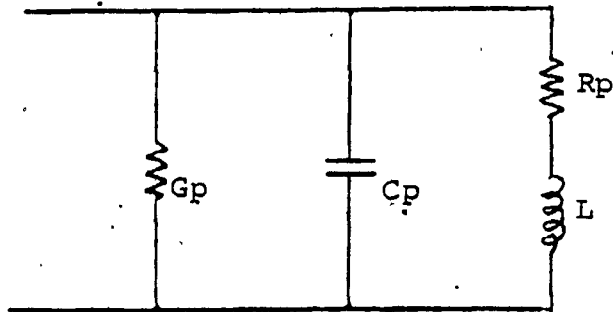


Fig. 3.7

Simulated inductor given by [67].

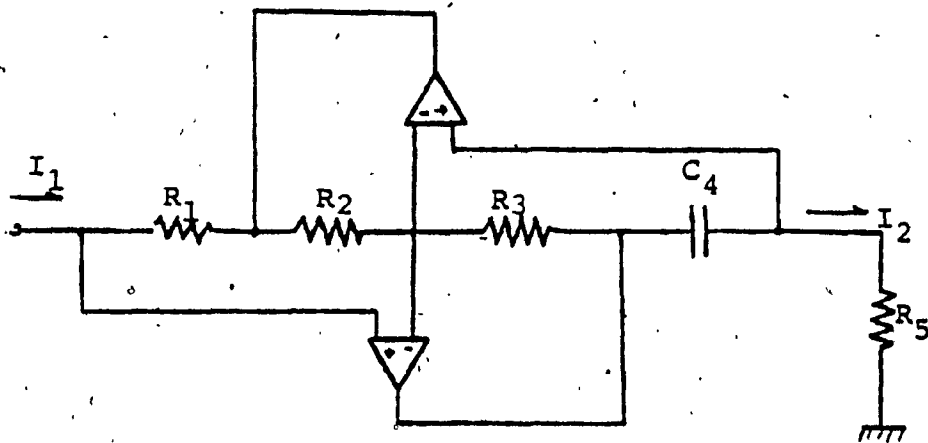


Fig. 3.8

The Antoniou GIC used to realize a simulated inductance

In this analysis all resistors were assumed equal. From the above parameters, L_0 represents the nominal inductance, and the rest represent parasitic elements due to imperfections of the operational amplifiers and load capacitor. Also the magnitudes of these elements depend on frequency (ie. gain bandwidth product of the amplifiers).

Therefore two simplified models were introduced [25], for better representation of the gyrator for low frequencies and high frequencies, as shown in Fig. 3.6.

The analysis of Ref. [25] is the most extensive one, compared to other reports up to date, because all the parasitic elements and non-ideal parameters, of an operational amplifier are taken into account.

A more simplified analysis is given by Ref. [67]. The GA type gyrator is analyzed and the following parasitic elements are reported.

$$G_p = \frac{2}{A_0 R_1} \left(1 + \frac{\omega^2}{A_0 \omega_0^2} \right) \quad (3.41)$$

$$C_p = 2(A_0 \omega_0 R_1)^{-1} \quad (3.42)$$

$$R_p = \frac{2R_1}{A_0} \left(1 + \frac{\omega^2}{A_0 (\omega_0)^2} \right) \left(1 - \frac{4\omega^2}{A_0 \omega_0} C_1 R_5 \right) \quad (3.43)$$

$$L = L_0 \left(1 + \frac{2}{A_0 \omega_0 C_1 R_5} \right) \quad (3.44)$$

This analysis assumes $R_2=R_3=R$, and

$$R_O \ll (R_1, R_2, R_3, R_5) \ll (R_D, R_C) \quad (3.45)$$

where

R_O is the output impedance of the operational amplifier.

R_D is the differential input impedance of the operational amplifier.

R_C is the common-mode impedance of the operational amplifier.

The presence of these parasitic elements raises design problems, which may be minimized by using as criterion the Q-factor for optimum design. The Q-factor of the simulated inductor with impedance Z_L is defined by

$$Q_L = \frac{\text{Im } Z_L}{\text{Re } Z_L} \quad (3.46)$$

The design is optimized by maximizing the Q-factor. For a given frequency f_k , the Q-factor is maximum if

$$R_1 = \omega_k L \left(1 + \frac{2f_k}{A_O f_O} \right) \quad (3.47)$$

$$C = \frac{1}{\omega_k R_S} \left(1 - \frac{4f_k}{A_O f_O} \right) \quad (3.48)$$

For this critical frequency f_k , a suitable value is chosen at which a high Q-factor is of prime importance. This is the case where the tolerance sensitivity of the filter is greatest and therefore component tolerances have

the maximum effect on attenuation distortion. This occurs at the frequency at which the attenuation curve has the steepest slope and the group delay is a maximum [6].

3.7 Effects of Finite Operational Amplifier's Gain

Above 50KHZ, the operational amplifier's gain can be approximated as

$$A(s) = \frac{A_0 \omega_c}{s} \quad \text{provided that } \omega \ll \omega_c \quad (3.49)$$

The input admittance of the GA type gyrator is given by [6]

$$Y_{IN} = \frac{I_1}{V_1} = \frac{I_2}{V_2} \frac{Y_1 Y_3}{Y_2 Y_4} \frac{1 + \frac{1}{A(s)} \left(1 + Y_4 \frac{V_2}{I_2}\right) + \frac{1}{A(s)} \frac{Y_2}{Y_3} \left(1 + Y_4 \frac{V_2}{I_2}\right) + \frac{1}{A^2(s)} \left(1 + \frac{Y_2}{Y_3}\right) \left(1 + Y_4 \frac{V_2}{I_2}\right)}{1 + \frac{1}{A(s)} \frac{Y_3}{Y_2} \left(1 + \frac{1}{Y_4} \frac{I_2}{V_2}\right) + \frac{1}{A(s)} \left(1 + \frac{1}{Y_4} \frac{I_2}{V_2}\right) + \frac{1}{A^2(s)} \left(1 + \frac{Y_3}{Y_2}\right) \left(1 + \frac{1}{Y_4} \frac{I_2}{V_2}\right)} \quad (3.50)$$

From the above approximation we can ignore the second order terms of A(s), and the input admittance of the gyrator becomes

Substituting equation (3.55) to equation (3.52) and (3.53)

we get

$$1 - 1 + Y_4 \frac{V_2}{I_2} - \frac{1}{Y_4} \frac{I_2}{V_2} = 0 \quad (3.56)$$

$$1 - 1 + Y_4 \frac{V_2}{I_2} - \frac{1}{Y_4} \frac{I_2}{V_2} = 0 \quad (3.57)$$

or

$$Y_4 \frac{V_2}{I_2} = \frac{1}{Y_4} \frac{I_2}{V_2}$$

which implies that

$$\frac{I_2}{V_2} = Y_4 \quad (3.58)$$

Eqn. (3.55) is easily satisfied by letting

$$Y_2 = Y_3 = g \quad (3.59)$$

where g is real.

In practice, second-order effects which were ignored in Eqn. (3.51) will dominate if $Y_2 = Y_3 = g$ [80]. However, Eqn. (3.58) is seldom satisfied, since $\frac{I_2}{V_2}$ has, in general, components orthogonal to Y_4 . Setting $Y_2 = Y_3$ in Eqn. (3.51) we get

$$Y_1 = \frac{I_1}{V_1} = \frac{I_2}{V_2} \frac{Y_1}{Y_4} \left[1 + j \left(\frac{2\omega}{\omega_c} \right) \left(Y_4 \frac{V_2}{I_2} - \frac{1}{Y_4} \frac{I_2}{V_2} \right) \right] \quad (3.60)$$

From the above equation one concludes that for best performance at the most critical frequency ω_{cf} (upper cut-off frequency of the band-pass filter) the quantity

$$Y_{IN} = \frac{I_1}{V_1} \approx \frac{I_2}{V_2} \frac{Y_1 Y_3}{Y_2 Y_4} \left[1 + j \left(\frac{\omega}{\omega_c} \right) \left(1 - \frac{Y_3}{Y_2} Y_4 \frac{V_2}{I_2} - \frac{Y_3}{Y_2 Y_4} \frac{I_2}{V_2} \right) + j \left(\frac{\omega}{\omega_c} \right) \times \left(\frac{Y_2}{Y_3} - 1 + \frac{Y_2 Y_4}{Y_3} \frac{V_2}{I_2} - \frac{1}{Y_4} \frac{I_2}{V_2} \right) \right] \quad (3.51)$$

In this analysis the two amplifiers are assumed to be identical. From equation (3.51) we see that for ideal performance of the gyrator, the imaginary part should be equal to zero. Thus, the following equalities should hold

$$1 - \frac{Y_3}{Y_2} + Y_4 \frac{V_2}{I_2} - \frac{Y_3}{Y_3 Y_4} \frac{I_2}{V_2} = 0 \quad (3.52)$$

$$\frac{Y_2}{Y_3} - 1 + \frac{Y_2 Y_4}{Y_3} \frac{V_2}{I_2} - \frac{1}{Y_4} \frac{I_2}{V_2} = 0 \quad (3.53)$$

Since in general $\frac{V_2}{I_2}$ is a function of frequency and takes on a complex value, then $1 + \frac{Y_3}{Y_2}$ must be linearly independent of

$$Y_4 \frac{V_2}{I_2} - \frac{Y_3}{Y_2 Y_4} \frac{I_2}{V_2} \quad (3.54)$$

Thus from equation (3.52) and (3.53) we conclude that it is necessary to have

$$1 - \frac{Y_3}{Y_2} = 0$$

which implies

$$Y_2 = Y_3 \quad (3.55)$$

Thus taking

$$\omega_{cf} C_4 = \left. \frac{I_2}{V_2} \right|_{\omega=\omega_{cf}} \quad (3.64)$$

minimizes M. Then the corresponding value for the GA type gyrator transfer function is

$$\frac{I_i}{V_1} = \frac{I_2}{V_2} \frac{Y_1}{Y_4} \left[\left(1 - \frac{4\omega}{\omega_c} \right) \cos \theta \right] \quad (3.65)$$

at $\omega = \omega_{cf}$

or

$$\left. \frac{I_1}{V_1} \right|_{\omega=\omega_{cf}} = \frac{Y_1 Y_5}{Y_4} \left(1 - \frac{4\omega}{\omega_c} \right) \quad (3.66)$$

since $\frac{I_2}{V_2} = Y_5$

Also

$$Y_1 = \frac{1}{R_1}, \quad Y_5 = \frac{1}{R_5} \quad \text{and} \quad Y_4 = j\omega C_4 \quad (\text{for GA type}) \quad (3.67)$$

At the frequency of interest the above equation becomes

$$\left. \frac{V_1}{I_1} \right|_{\omega=\omega_{cf}} = j\omega R_1 R_5 C_4 \left(1 + \frac{4\omega}{\omega_c} \right) \quad (3.68)$$

$$M = \left(Y_4 \frac{V_2}{I_2} - \frac{1}{Y_4} \frac{I_2}{V_2} \right)$$

should be as small as possible, because at this frequency, the group delay has its greatest value.

Letting

$$\left. \frac{V_2}{I_2} \right|_{\omega = \omega_{cf}} = Ae^{j\theta} \quad (3.61)$$

it follows that we require

$$M = Y_4 Ae^{j\theta} - \frac{1}{Y_4 Ae^{j\theta}}$$

to be as small as possible.

The type of gyrator used for this filter is type GA which requires that $Y_4 = j \omega C_4$, where C_4 is real.

Therefore

$$M = j\omega_{cf} C_4 A(s) e^{j\theta} + \frac{j e^{-j\theta}}{\omega_{cf} C_4 A(s)} \quad (3.62)$$

which implies that

$$M = j \left(\frac{1}{\omega_{cf} C_4 A(s)} + \omega_{cf} C_4 A(s) \right) \cos\theta + \left(\frac{1}{\omega_{cf} C_4 A(s)} - \omega_{cf} C_4 A(s) \right) \sin\theta \quad (3.63)$$

Minimization of the above equation occurs when

$$\omega_{cf} C_4 = \frac{1}{A(s)}$$

where the second term reduces to zero.

From the above equation we see that the input inductance has an infinite Q factor (since the real part of the equation is zero), but undergoes a deviation in value, and is given by

$$\frac{\Delta L}{L} \Big|_{\omega=\omega_{cf}} = \frac{4\omega}{\omega_c} \quad (3.69)$$

This equation implies that the deviation of the inductance value is strictly dependent on the gain-bandwidth product of the operational amplifier. The higher the gain-bandwidth product of the operational amplifiers the lower the deviation of the inductance. To minimize M (optimization of GA type of gyrator) we let

$$\omega_{cf} C_4 = \left| \frac{I_2}{\sqrt{2}} \right|_{\omega=\omega_{cf}} = \frac{1}{R_5} \quad (3.70)$$

or

$$\omega_{cf} C_4 R_5 = 1$$

Thus eqn. (3.68) becomes

$$\frac{V_1}{I_1} \Big|_{\omega=\omega_{cf}} = jR_1 \left(1 + \frac{4\omega}{\omega_c} \right) \quad (3.71)$$

This equation also suggests the use of R_1 to adjust or to trim the value of the input inductance, from the deviation due to finite gain-bandwidth product of the operational amplifiers.

CHAPTER 4

IMPLEMENTATION AND TUNABILITY OF BAND-PASS FILTER

4.1 Introduction

The value of a simulated inductance is determined by the value of five passive components in the ideal case. The inductance is typically described by an equation of the form: $L = R_1 R_3 R_5 C_4 / R_2$. Thus, the percentage errors of the components add up. If each component has a tolerance of $\pm 1\%$, L has a maximum error of 5%. In practice, the component errors will not all have the same sign or magnitude, so the error in L will probably be considerably smaller. In any event, it is easy to adjust L by means of potentiometer, in place of R_1 as Eqn. (3.71) suggests. The tunability of the filter was relatively simple. Two different methods were used with the same results.

4.2 Band-Pass Filter Using Gytrators

The band-pass filter was implemented with the replacement of all inductors with multi-inductor network. The two π inductor sections were simulated with two gyrators, each one sharing one resistor to reduce the number of gyrators used. The four gyrators used were identical with optimized component values as follows.

$$R_2 = R_3 = 4.99K\Omega \pm 1\% \quad (4.1)$$

for optimum performance. The second of these equations suggests that the lower the gain of the operational amplifier the higher the value of the capacitor used (for a certain frequency), and less influence of the parasitic capacitance of the gyrator.

A value of 3.6nF was chosen for C_4 . Then R_5 is determined as

$$R_5 = \frac{1}{\omega C_4} = \frac{1}{2\pi \times 110 \times 10^3 \times 3,600 \times 10^{-12}} = 402\Omega \quad (4.8)$$

The value of R_5 then determines the value of the sharing resistance, R_6 which is analogous to the ratio

$$\frac{L_1}{L_2} = \frac{R_5}{R_6} \quad (4.9)$$

From the above analogue the only unknown value is R_6 .

Therefore

$$R_6 = \frac{R_5 L_2}{L_1} = \frac{402 \times 11.874599 \times 10^{-3}}{0.512982 \times 10^{-3}} = 9,305.56\Omega \quad (4.10)$$

$R_6 = 9.31\text{K} \pm 1\%$ was used, as the closest standard value.

At the beginning the operational amplifier used was the Harris type HA4622, dual-in-line 14 pin package containing 4 operational amplifiers. The gain bandwidth product of this type is 70MHz which was suitable for the band-pass filter implementation. The filter was implemented but it was unstable. The reason for instability was the operational

for Q enhancement with respect to amplifier bandwidth [23]. The Q factor has been derived and is given by Ref. [80] as

$$Q(\omega) = \frac{A_o}{2} \cdot \frac{1}{\omega RC + \frac{1}{\omega RC}} \quad (4.2)$$

In the above equation resistances R_1, R_2, R_3, R_5 were assumed all equal, therefore $L_o = CR^2$.

Hence

$$Q(\omega) = \frac{A_o}{2} \cdot \frac{1}{\frac{\omega L_o}{R} + \frac{R}{\omega L_o}} \quad (4.3)$$

This equation suggests that for a maximum Q at a given frequency ω_c

$$R = \omega_c L_o \quad (4.4)$$

This frequency in this band-pass filter is the upper cut-off frequency equal to 110KHZ therefore the value of R is

$$R = 2\pi \times 110 \times 10^3 \times 0.512982 \times 10^{-3} = 354.54 \Omega \quad (4.5)$$

This value was used for resistor R_1 , and since with this resistor we control the value of the inductance, as equation (3.71) suggests, then a potentiometer was used for trimming purposes.

Also from Eqn. (3.63), (3.70) we have

$$W_c C_4 R_5 = 1 \quad (4.6)$$

$$W_c C_4 = \frac{1}{A(s)} \quad (4.7)$$

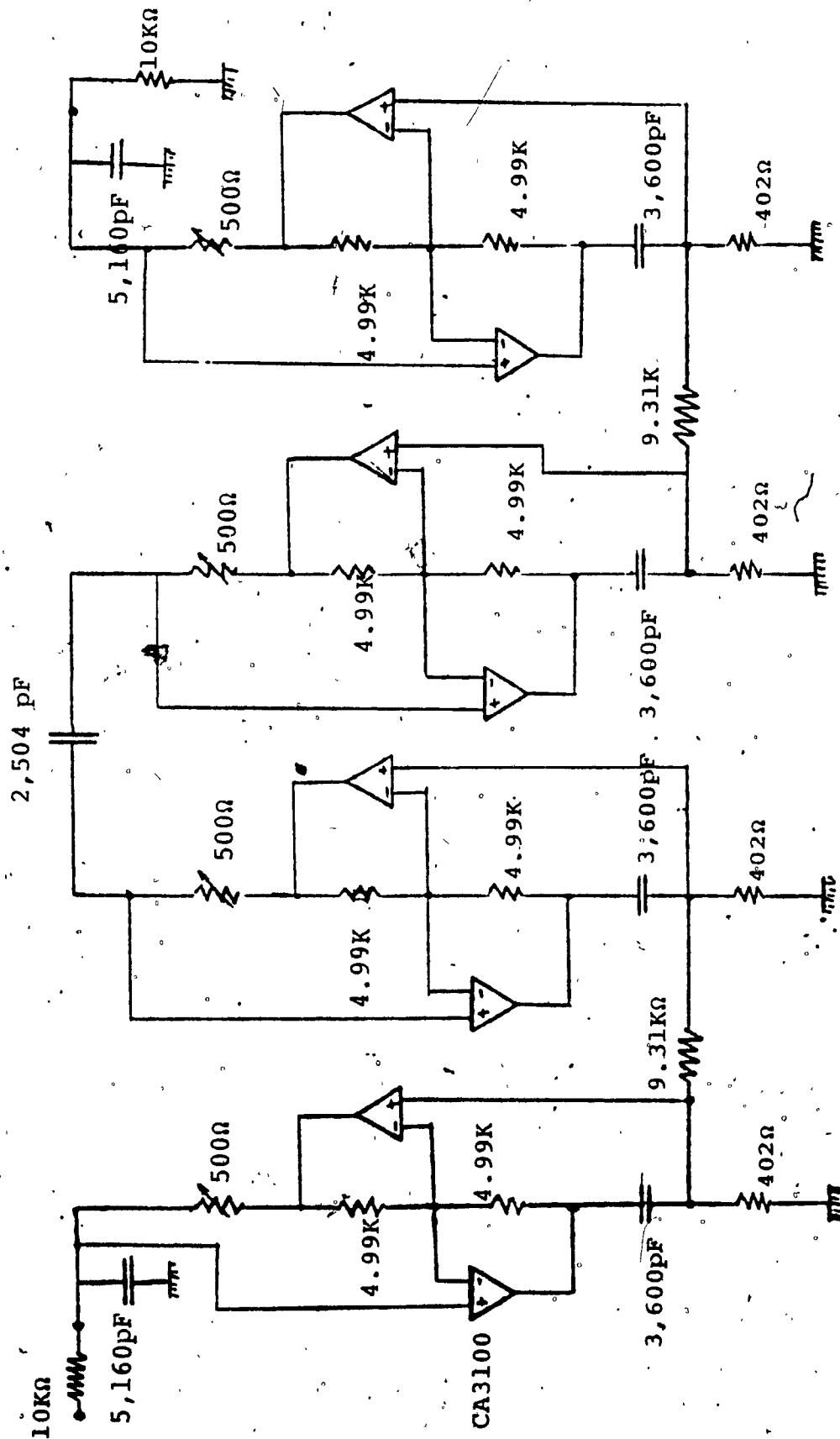


Fig. 4.1
Band-pass filter (realized)

amplifier itself, because this type of operational amplifier, besides the excellent parameters, is unstable for a gain less than five. For the implementation of gyrator the operational amplifier must be stable for a gain of unity.

The RCA operational amplifier, CA3100T was then used. This amplifier has a gain bandwidth product of 38MHZ, and unity gain stability. The filter is shown in Fig. 4.1 with actual values.

4.3 Tuning the Band-Pass Filter

Tuning of the filter was done as follows: through a $10M\Omega$ resistor, we feed the signal to the parallel LC circuit, at center frequency of 100KHZ, and we trim the 500Ω potentiometer to achieve resonance at the center frequency, as in Fig. 4.2.

Since all the shunt inductors have the same value, the adjustment for each gyrator is very easy and accordingly the band-pass filter is tuned without any other difficulty, by interconnecting the two sharing resistors,

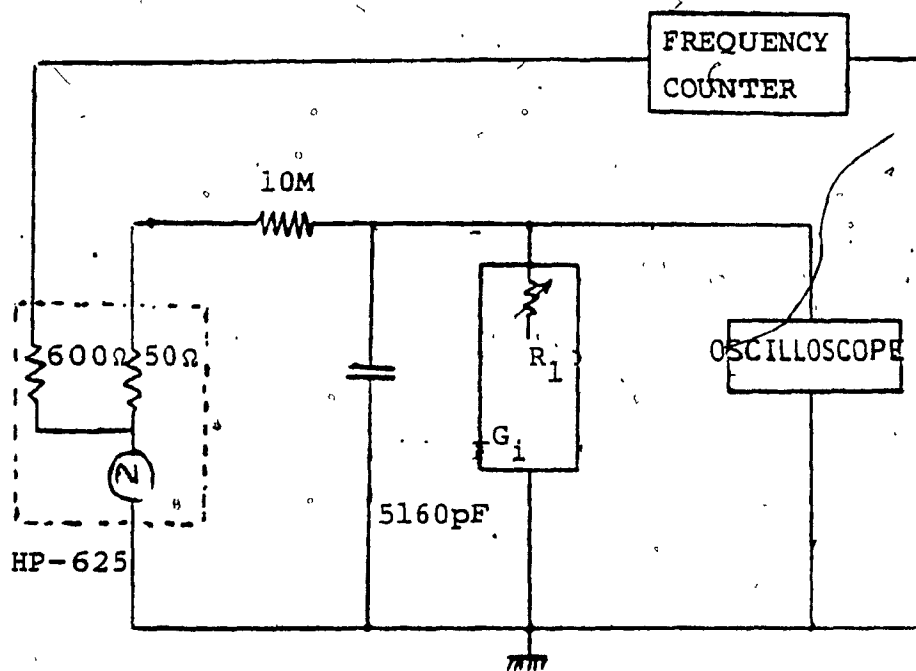


Fig. 4.2

Tunning gyator (G_i).

C_2 , input and output impedances.

Another way of tuning this filter is by using Lissajous figures. Since this filter is designed symmetrical, the tuning can be done in two parts by disconnecting capacitor C_2 in Fig. 4.3.

Using point A as the output, the first gyrator is set by shorting point B to ground and adjusting R_1 to achieve resonance at the center frequency. This results into 0° phase-shift relative to the source. Then we disconnect point B from ground, and tune R_1 of the second gyrator for 90° phase-shift at the output. We follow the same procedure for the second part of the filter. Then by connecting back capacitor C_2 , the filter is tuned with an accuracy better than 2° .

4.4 Parasitic Effects

The band-pass filter after tuning had a response far from ideal. The deviation from the ideal response was due to the parasitic elements introduced by Ref. [24] as G_{p_3} , r_{p_5} , L_p , and C_p . Since the values of all, resistors, capacitor, and various parameters of the operational amplifier (for each gyrator) were established, the parasitic elements were calculated as follows

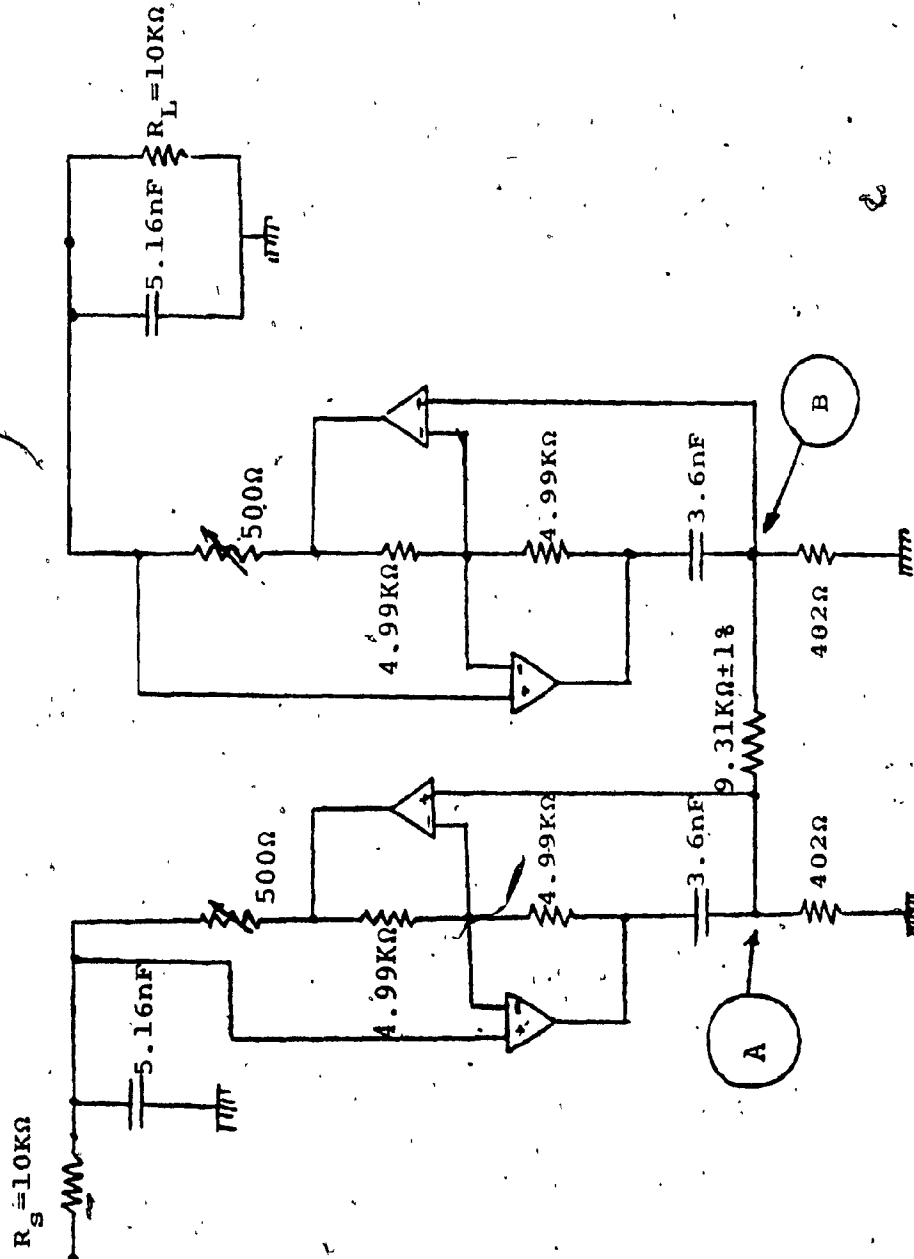


Fig. 4.3

Tuning band-pass filter

$$G_{P_3} = \frac{R_2}{R_1} \left(\frac{1}{R_3 A_O} + \frac{1}{R_2 A_O} \right) = \frac{2}{R_1 A_O} = 5.6497 \times 10^{-6} \text{ Mho}$$

or

$$\frac{1}{G_{P_3}} = R_3 = 177 \text{ K}\Omega$$

$$r_{P_5} = \frac{2\omega^2}{A_O^2 \omega^2} (R + 6R_O) = \frac{R_1}{R_2} \left(\frac{R_2}{A_O} + \frac{R_3}{A_O} \right) = \frac{R_1 (R_2 + R_3)}{R_2 A_O} = 0.709 \text{ m}\Omega \quad (4.11)$$

$$L_p = \frac{R_1 (R_2 R_3)}{R_2 B} = 0.003 \text{ }\mu\text{H} \quad (4.12)$$

$$C_p = \frac{R_2}{R_1} \left(\frac{1}{R_3 B} + \frac{1}{R_2 B} \right) = \frac{2}{R_1 B} = 23 \text{ pF} \quad (4.13)$$

From the above calculations we see that the only significant parasitic element is capacitance C_p . This parasitic capacitance affects the quality factor Q_L of the simulated inductor. This quality factor is the ratio of the capacitor C_4 to the parasitic capacitance C_p , Ref. [6].

$$Q_L = \frac{C_4}{C_p} = \frac{3,600 \text{ pF}}{23 \text{ pF}} = 156.5 \quad (4.14)$$

Two different compensation techniques have been introduced for elimination (or reduction) of this parasitic capacitance. Ref. [25] suggests the use of a capacitor C_c with a value as

$$C_c = \frac{2R + R_O}{A_O \omega_o R^2} \quad (4.15)$$

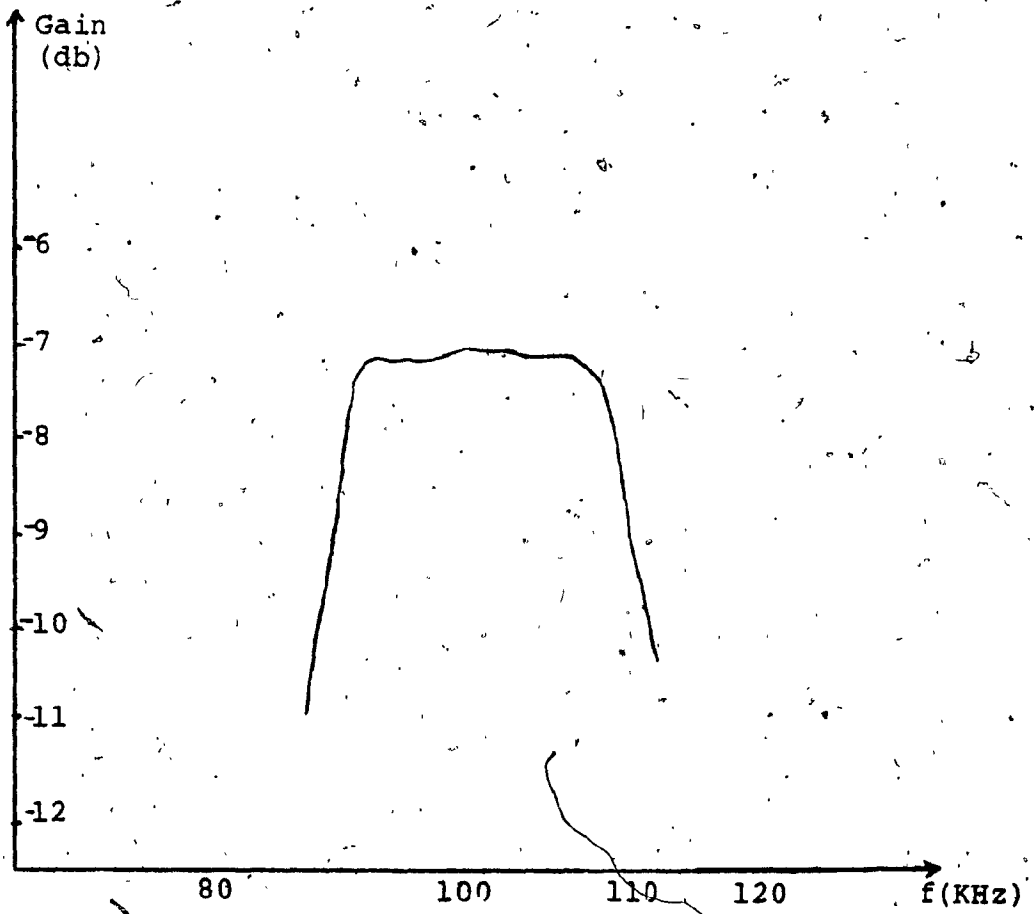


Fig. 4.4
Frequency response of active Band-pass filter

where $R = R_2 = R_3$

Ref. [6] suggests the use of a resistor R_c with a value as

$$R_c = R \frac{C_4}{C_p} \quad (4.16)$$

where $R = R_2 = R_3$

Both compensating elements are inserted between the common inverting input terminals of the operational amplifiers to ground.

Both methods were tested and in my opinion the use of a compensating variable resistor is better, because the tuning process is faster than using capacitor. At the frequency of 100KHZ, the simulated inductance is also sensitive to stray capacitances, and a good layout is very important for best results.

With the use of compensating resistors the response of the band-pass filter improved significantly and the aim of this report was achieved.

CONCLUSIONS

The feasibility of implementing high-Q, active, band-pass filters with gyrators has been studied. The design is based on a suitably transformed passive filter network, by replacing the inductors by capacitively-terminated gyrators. With the use of gyrators instead of inductors, the filter preserves its insensitivity to component variations, and since the gyrator is an active circuit it does not add dissipative elements to the filter.

From the various types of gyrators that have appeared in the literature, the Antoniou type has been investigated and analysed. The main sources of errors are the imperfection of the operational amplifiers used due to limited gain-bandwidth product. From all the parasitic elements introduced, the parasitic capacitor is the most important one. Optimization of the gyrator consists of the elimination of this parasitic capacitance which is done by two different approaches. Both methods improved the performance of the gyrators, and a frequency response has been achieved for the band-pass filter which is close to the desirable one.

REFERENCES

- [1]. Handbook on Electrical Filters, "Synthesis, Design and Applications", White Electromagnetics Inc. 1963.
- [2]. Swamy, M.N.S., "Active and Passive Filters", Notes Concordia University.
- [3]. Stewart, John L., "Circuit Theory and Design", John Wiley & Sons, Inc., New York, 1956.
- [4]. Mitra, S.K., "Analysis and Synthesis of Linear Active Networks", John Wiley & Sons, Inc., New York, 1969.
- [5]. Antoniou, A., "Realization of Gyration using Operational Amplifiers and their use in RC-Active Network Synthesis", Proc. IEE, Vol. 116, Nov. 1969, pp. 1838-1850.
- [6]. Martin, K. and Sedra, A., "Optimum Design of Active Filters using the Generalized Immitance Converters", IEEE Trans. on Circuit and Systems, Vol. CAS-24, No. 9, Sept. 1977, pp. 495-503.
- [7]. Huelsman, L.P., "Active Filters", McGraw-Hill Book Company, New York, 1970.
- [8]. Voorman, Hans O. and Biesheuvel, Arnold, "An Electronic Gyrator", IEEE Journal of Solid State Circuits, Vol. SC-7, No. 6, Dec. 1972, pp. 469-474.
- [9]. Tellegen, B.D.H., "The Gyrator, A New Electric Network Element", Philips Res. Rep., Vol. 3, April 1948, pp. 81-101.

- [10]. Haykin, S.S., "Synthesis of RC Active Filter Networks", McGraw-Hill, London, 1969.
- [11]. Budac, A., "Passive and Active Network Analysis and Synthesis", Houghton Mifflin Co., 1974.
- [12]. Heinlein, W.E., Holmes, W.H., "Active Filters for Integrated Circuits", Oldenbourg Verlag GmbH, Munchen, 1974.
- [13]. Antoniou, "New Gyrator Circuits Obtained by Using Nullors", Electronics Letters, Vol. 4, No. 5, March 8, 1968, pp. 87-88.
- [14]. Antoniou, A., "Novel RC-Active-Network Synthesis Using Generalized Immitance Converters", IEEE Trans. Circuit Theory, Vol. CT-17, May 1970, pp. 212-217.
- [15]. Bhattacharyya, B.B., "Active Filter Design", Notes, Concordia University.
- [16]. Voorman, J.O., "The Adaptive Gyrator" IEEE Proc. ISCAS/76, pp. 34-37.
- [17]. Riordan, R.H.S., "Simulated Inductors Using Differential Amplifiers", Electronics Letters, Vol. 3, Feb. 1967, pp. 50-51.
- [18]. Gorski-Popiel, J., "RC-Active Synthesis using Positive-Immitance Converters", Electronics Letters, Vol. 3, Aug. 1967, pp. 381-382.

- [26]. Antoniou, A., "Influence of Ambient-Temperature Variations in Two Gyrator Circuits", Proc. IEEE, Vol. 123, No. 6, June 1976, pp. 490-494.
- [27]. Thimm, R., "Realization of Active Bandpass Filters using Nonideal Impedance Converters", IEEE Proc. ISCAS/76, pp. 73-77.
- [28]. Antoniou, A., "Gyrators using Operational Amplifiers", Electronics Letters, August 1967, Vol. 3, No. 8, pp. 350-352.
- [29]. Silva, M.M., "On the Realization of One Nullor Gyrators", IEEE Proc. 1975 ISCAS, pp. 273-276.
- [30]. Panzer, K., "Active Bandpass Filter with a Minimum Number of Capacitors using Frequency Dependent Negative-Resistances and a Gyrator", IEEE Proc. ISCAS/76, pp. 38-40.
- [31]. Soundararajan, K. and Ramakrishna, K., "Characteristics of Nonideal Operational Amplifiers", IEEE Trans. Circuits and Systems, Vol. CAS-21, No. 1, January 1974, pp. 69-75.
- [32]. Brackett, Peter O. and Sedra, Adel S., "Active Compensation for High-Frequency Effects in Op. Amp. Circuits with Applications to Active RC Filters", IEEE Trans. Circuits and Systems, Vol. CAS-23, No. 2, February 1976, pp. 68-72.

- [19]. Rao, T.N., and Newcomb, R.W., "Direct-Coupled Gyrator Suitable for Integrated Circuits and Time Variation", Electronics Letters, Vol. 2, July 1966, pp. 250.
- [20]. Bruton, L.T., "Nonideal Performance of Two-Amplifier Positive Impedance Converters", IEEE Trans. Circuit Theory, Vol. CT-17, Nov. 1970, pp. 541-548.
- [21]. Lynch, T.H., "The Right Gyrator Trims the Fat Off Active Filters", Electronics Magazine, July 21, 1977, pp. 100-104.
- [22]. Orchard, H.J., Sheahan, D.F., "Inductorless Band-pass Filters", IEEE J. Solid State Circuits, Vol. SC-5, June 1970, pp. 108-118.
- [23]. Bruton, L.T., "Multiple-Amplifier RC-Active Filter Design with Emphasis on GIC Realizations", IEEE Trans. on Circuits and Systems, Vol. CAS-25, No. 10, Oct. 1978, pp. 830-845.
- [24]. Antoniou, A., and Naidu, K.S., "Modeling of a Gyrator Circuit", IEEE Trans. on Circuit Theory, Vol. CT-20, No. 5, Sept. 1973, pp. 533-540.
- [25]. Antoniou, A. and Naidu, K.S., "A Compensation Technique for a Gyrator and its Use in the Design of a Channel-Bank Filter", IEEE Trans. on Circuits and Systems, Vol. CAS-22, No. 4, April 1975, pp. 316-323.

- [33]. Moschytz, G.S., "The Operational Amplifier in Linear Active Networks", IEEE Spectrum, Vol. 7, January 1970, pp. 42-50.
- [34]. Solomon, James E., "The Monolithic Op. Ampl: A Tutorial Study", IEEE J. Solid-State Circuits, Vol. SC-9, December 1974, pp. 314-332.
- [35]. Gray, Paul R. and Mayer, Robert G., "Recent Advances in Monolithic Operational Amplifier Design", IEEE Trans. Circuits Syst., Vol. CAS-21, May 1974, pp. 317-327.
- [36]. Van Kessel, T.J., "An Integrated Operational Amplifier with Novel HF Behaviour", IEEE J. Solid-State Circuits, Vol. SC-3, December 1968, pp. 348-352.
- [37]. Van De Plassche, Rudy, "A Wide-Band Operational Amplifier with a new Output Stage and a Simple Frequency Compensation", IEEE J. Solid-State Circuits, Vol. SC-6, Dec. 1971, pp. 347-352.
- [38]. Hearn, William E., "Fast Slewing Monolithic Operational Amplifier", IEEE J. Solid-State Circuits, Vol. SC-6, Feb. 1971, pp. 20-24.
- [39]. Graeme, J.G. and Tobey, G.E., Huelsman, L.P., "Operational Amplifier, Design and Applications", McGraw-Hill Book Company, 1974, Burr-Brown Research Corporation.
- [40]. Ramakrishna, K., Soundarajan, K., Aatre, V.K., "Effect of Amplifier Imperfections on Active Networks", IEEE

Trans on Circuits and Systems, Vol. CAS-26, No. 11,
November 1979, pp. 922-931.

- [41]. Bruton, L.T. and Haase, A.B., "Sensitivity of Generalized Immitance Converter-Embedded Ladder Structures", IEEE Trans. on Circuits and Systems, Vol. CAS-21, No. 2, March 1974, pp. 245-250.
- [42]. Akerberg, D. and Mossberg, K., "A Versatile Active RC Building Block with Inherent Compensation for the Finite Bandwidth of the Amplifier", IEEE Trans. on Circuits and Systems, Vol. CAS-21, January 1974, pp. 75-78.
- [43]. Bruton, L.T., "Sensitivity Comparison of High-Q Second Order Active Filter Synthesis Technique", IEEE Trans. on Circuits and Systems, Vol. CAS-22, No. 1, January 1975, pp. 32-38.
- [44]. Srinivasagopalan, R., Martens, G.O., "A Comparison of a Class of Active Filters with Respect to the Operational Amplifier Gain-Bandwidth Product", IEEE Trans. on Circuits and Systems, Vol. CAS-21, No. 3, May 1974, pp. 377-381.
- [45]. Strycula, E.C., and Bose, N.K., "Theory and Applications of Simultaneous Realization of Transfer and Sensitivity Functions", IEEE Trans. on Circuits and Systems, Vol. CAS-21, No. 3, May 1974, pp. 382-387.

- [46]. Schaumann, Rolf, "Low-Sensitivity High-Frequency Tunable Active Filter without External Capacitors", IEEE Trans. on Circuits and Systems, Vol. CAS-22, No. 1, January 1975, pp. 39-44.
- [47]. Geffe, Philip R., "Exact Synthesis with Real Amplifiers" IEEE Trans. on Circuits and Systems, Vol. CAS-21, No. 3, May 1974, pp. 369-376.
- [48]. Moschytz, G.S., Horn, Peter, "Reducing Nonideal Op-Ampl. Effects in Active Filters by Minimizing the Gain-Sensitivity Product (GSP)", IEEE Trans. on Circuits and Systems, Vol. CAS-24, No. 8, August 1977, pp. 437-445.
- [49]. Sedra, Adel S., Espinoza, Juan L., "Sensitivity and Frequency Limitations of Biquadratic Active Filters", IEEE Trans. on Circuits and Systems, Vol. CAS-22, No. 2, February 1975, pp. 122-130.
- [50]. Allen, Philip E., "A Model for Slew-Induced Distortion in Single Amplifier Active Filters", IEEE Trans. on Circuits and Systems, Vol. CAS-25, No. 8, August 1978, pp. 565-572.
- [51]. Atiya, F.S., "The Composite Active Filter: A Combined Wave-Active and Gyrator-C Filter", IEEE Trans. on Circuits and Systems, Vol. CAS-25, No. 8, August 1978, pp. 573-579.
- [52]. Saraga, W., Haigh, D.G., and Barker, R.G., "Micro-electronic Active-RC Channel Bandpass Filters in the

- No. 10, October 1979, pp. 892-893.
- [59]. Soliman, A.M., Ismail, M., "Passive Compensation of Op.-Amp. VCVS and Weighted Summer Building Blocks", IEEE Trans. on Circuits and Systems, Vol. CAS-26, No. 10, October 1979, pp. 898-900.
- [60]. Geiger, R.L., Budak, A., "Active Filters with Zero Amplifier Sensitivity", IEEE Trans. on Circuits and Systems, Vol. CAS-26, April 1979, pp. 277-288.
- [61]. Soliman, A.M., Ismail, M., "Active Compensation of Op-Amps", IEEE Trans. on Circuits and Systems, Vol. CAS-26, No. 2, February 1979, pp. 112-117.
- [62]. Su, Kendall L., "Active Network Synthesis", McGraw-Hill Inc. 1965.
- [63]. Sun, Hun H., "Synthesis of RC Networks", Hayden Book Company Inc. 1967.
- [64]. Inigo, Rafael M., "Active Filter Realization using Finite-Gain Voltage Amplifiers", IEEE Trans. Circuit Theory, Vol. CT: 17, Aug. 1970, pp. 445-448.
- [65]. Sallen, R.P. and Key, E.L., "A Practical Method of Designing RC Active Filters", IRE Trans. Circuit Theory, Vol. CT.2, March 1955, pp. 74-85.
- [66] Kerwin, W.J., Huelsman, L.P., "The Design of High Performance Active RC Band-Pass Filters", IEEE Int. Conv. Rec. Vol. 14, Part 10, 1966, pp. 74-80

Frequency Range 60-108KHz for FDM SSB Telephone Systems", IEEE Trans. on Systems and Circuits, Vol. CAS-25, No. 12, December 1978, pp. 1022-1031.

- [53]. Silva, M.M., "On the Realization of Immitance Inverters with a Minimum Number of Active Components", IEEE Trans. on Circuits and Systems, Vol. CAS-26, No. 11, November 1979, pp. 931-935.
- [54]. Laker, K.R., Schaumann, R., and Ghausi, M.S., "Multiple-Loop Feedback Topologies for the Design of Low-Sensitivity Active Filters", IEEE Trans. on Circuits and Systems, Vol. CAS-26, No. 1, January 1979, pp. 1-21.
- [55]. Horn, P. and Moschytz, G.S., "Active RC Single Op-Amp. Design of Driving-Point Impedances", IEEE Trans. on Circuits and Systems, Vol. CAS-26, No. 1, January 1979, pp. 22-30.
- [56]. Allen, P.E., Cavin III, R.K., and Kwou, C.G., "Frequency Domain Analysis for Operational Amplifier Macromodels", IEEE Trans. on Circuits and Systems, Vol. CAS-26, No. 9, September 1979, pp. 693-699.
- [57]. Sanchez-Silencio, E., and Masecuski, M.L., "A Nonideal Macromodel of Operational Amplifier in the Frequency Domain", IEEE Trans. on Circuits and Systems, Vol. CAS-26, No. 6, June 1979, pp. 395-402.
- [58]. Patranabis, D, Tripathi, M.P., and Roy, S.B., "A New Approach for Lossless Floating Inductor Realization", IEEE Trans. on Circuits and Systems, Vol. CAS-26,

- [67]. Thimm, R., "Active Filters for Channel Translating Equipment", Electrical Communication, Vol. 52, No. 2, 1977, pp. 130-136.
- [68]. Bhattacharyya, B.B., Mikhael, W.B., and Antoniou, A., "Design of RC-Active Networks using Generalized-Immittance Converters, Journal of the Franklin Institute, Vol. 297, No. 1, Jan. 1974, pp. 45-50.
- [69]. Antoniou, A., "Floating Negative-Imepdance Converters", IEEE Trans. on Circuit Theory, March 1972, pp. 209-212.
- [70]. Antoniou, A., "Bandpass Transformation and Realization using Frequency-Dependent Negative-Resistance Elements", IEEE Trans. on Circuit Theory, March 1971, pp. 297-298.
- [71]. Roy, S.C. Dutta, Ahmed, M.Taj, "Synthesis of RC Active Networks using Nonideal Simulated Inductance", IEEE Trans. on Circuits and Systems, Vol. CAS-21, No. 2, March 1974, pp. 250-251.
- [72]. Bruton, L.T., "Network Transfer Functions using the Concept of Frequency-Dependent Negative Resistance", IEEE Trans. Circuit Theory, Vol. CT-16, August 1969, pp. 406-408.
- [73]. Holmes, W.H., Heinlein, W.E., and Grutzmann, S., "Sharp-cutoff Low-pass Filters using Floating Gytrators", IEEE J. Solid-State Circuits, Vol. SC-4, Feb. 1969, pp. 38-50.

- [74]. Anandamohan, P.V., "A Novel Bandpass Filter using the Amplifier Pole", IEEE Journal of Solid-State Circuits, Vol. SC-14, No. 3, June 1979, pp. 649-651.
- [75]. Abougabal, M.S., Bhattacharyya, B.B., and Swamy, M.N.S., "An Optimal Design of RC Active Filters using Grounded Capacitors", IEEE Trans. Circuit Theory and Applications Vol. 6, 1978, pp. 31-40.
- [76]. Mikhael, W.B., and Bhattacharyya, B.B., "Stability Properties of Some Active Realizations", Electronics Letters, Vol. 8, No. 11, 1972 (reprint).
- [77]. Mikhael, W.B., Bhattacharyya, B.B., "A Practical Design for Insensitive RC-Active Filters", IEEE Trans. on Circuits and Systems, Vol. CAS-22, No. 5, May 1975, pp. 407-415.
- [78]. Natarajan, S., Bhattacharyya, B.B., "Optimization of RC Active Filters for Extended Bandwidth Operation", Proceedings of the IEEE, Vol. 66, No. 2, Feb. 1978, pp. 260-261.
- [79]. Bruton, L.T., "Nonideal Performance of a Class of Positive Immittance Converters", IEEE Trans. on Circuits Theory, Nov. 1969, pp. 572-573.
- [80]. Valihora, J., Lim, J.T., "The Feasibility of Active Filtering in Frequency Division Multiplex Systems", Proceedings, 1974, IEEE International Symposium on Circuits and Systems, April 22-25, 1974, pp. 121-125.

pp. 719-721.

[88]. Holmes, W.H., "On Inverters and Converters", IEEE Trans. on Circuit Theory, Nov. 1971, pp. 723-726.

[89]. Muller, Jochen H.W., "Hybrid Integrated Gyrator in Dual-In-Line Package for Universal Application", IEEE Trans. on Circuit Theory, Nov. 1971, pp. 726-728.

- [81]. Brierley, H.G., "The Frequency Limitations of a Gyrator Circuit", The Radio and Electronic Engineer, Vol. 43, No. 11, Nov. 1973, pp. 695-702.
- [82]. Moulding, K.W., and Wilson, A., "A Fully Integrated Five-Gyrator Filter at Video Frequencies", IEEE Journal of Solid-State Circuits, Vol. SC-13, No. 3, June 1978.
- [83]. Ibrahim, M. Marzouk, "Frequency Performance of a Gyrator Circuit with BP-Applications", 1978 IEEE International Symposium on Circuits and Systems Proceeding, Rousevelt Hotel, New York, N.Y., May 17-19, 1978, pp. 860-861.
- [84]. Holmes, W.H., "A New Method of Gyrator-RC Filter Synthesis", Proceedings of the IEEE, October 1966, pp. 1459-1460.
- [85]. Ramsey, W.T., "Highpass and Bandpass Filters using Single-Amplifier Simulated Inductors", 1978 IEEE International Symposium on Circuits and Systems Proceedings, Rousevelt Hotel, New York, N.Y., May 17-19, 1978, pp. 855-859.
- [86]. Huelsman, L.P., "The Compensation of Negative-Immitance Converters", Proceedings of the IEEE, July 1976, pp. 1015-1016.
- [87]. Trimmel, H.R., Heinlein, W.E., "Fully Floating Chain-Type Gyrator Circuit using Operational Transconductance Amplifiers", IEEE Trans. on Circuit Theory, Nov. 1971,